Supplemental Information

A Strong Organic Electron Donor Incorporating Highly π-Donating Triphenylphosphonium Ylidyl Substituents

Morgan M. Burgoyne, Thomas M. MacDougall, Zachary N. Haines, Jordan W. Conrad, Larry A. Calhoun, Andreas Decken and C. Adam Dyker*

Department of Chemistry, University of New Brunswick, Fredericton, New Brunswick, E3B 5A3 (Canada); E-mail: cadyker@unb.ca

Contents:

List of Figures:

NMR Spectra

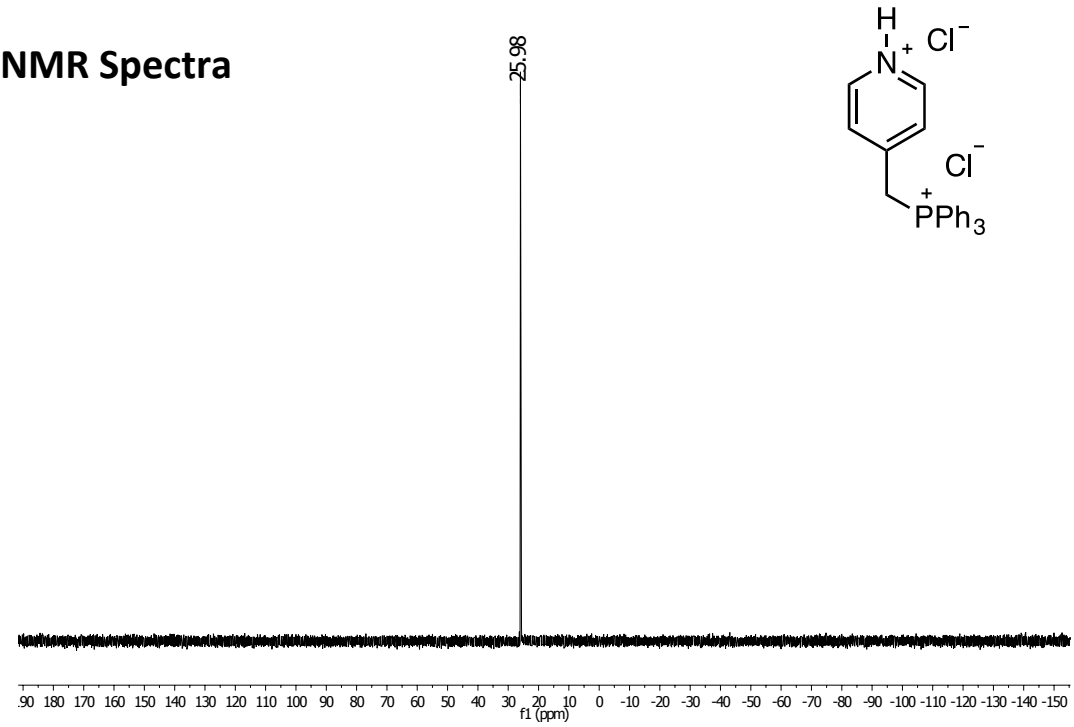

Figure S1 ^{31}P NMR spectrum of **2** in $CDCl_3$.

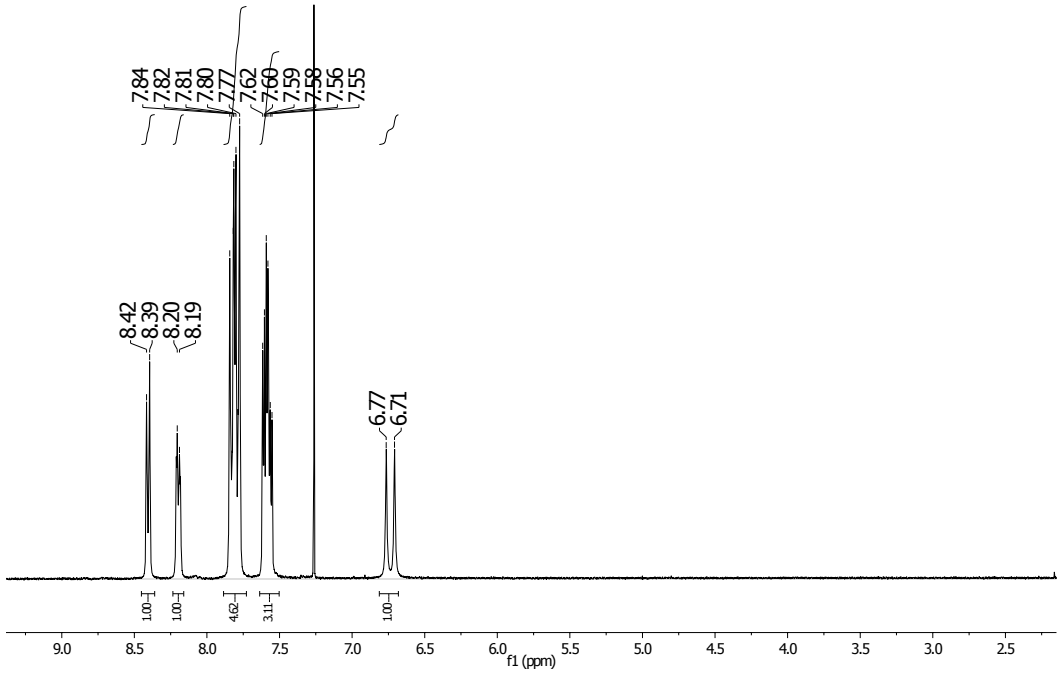

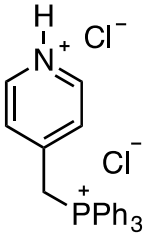

Figure S2 ^{1}H NMR spectrum of **2** in $CDCl_3$.

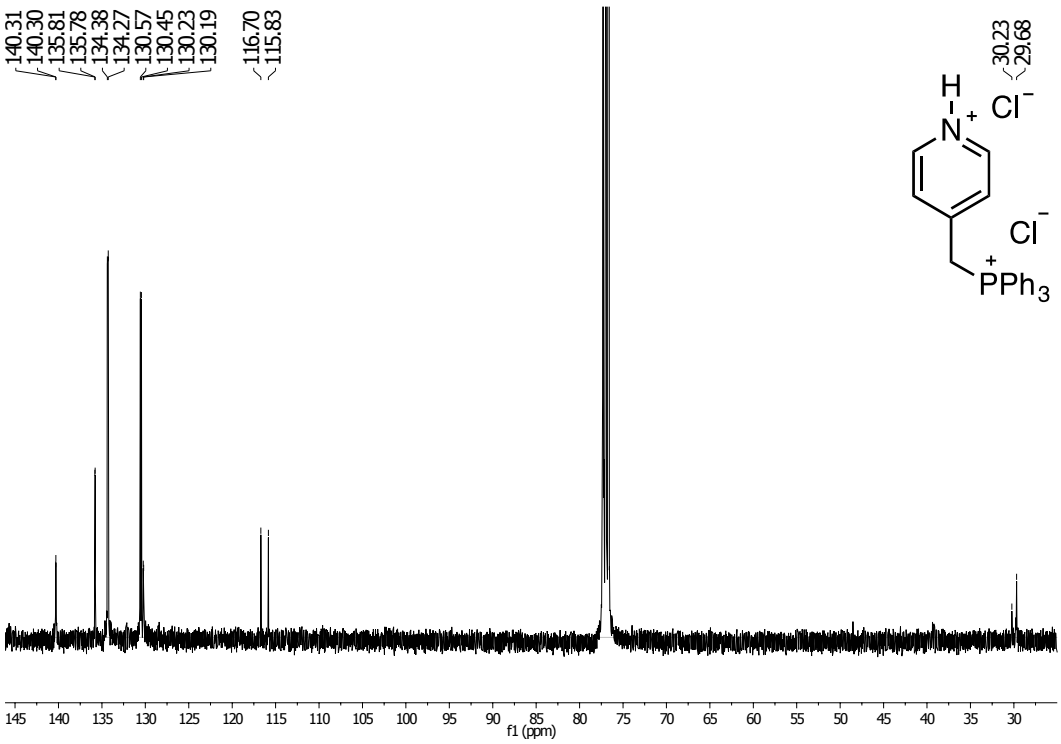

Figure S3 ^{13}C NMR spectrum of **2** in $CDCl_3$.

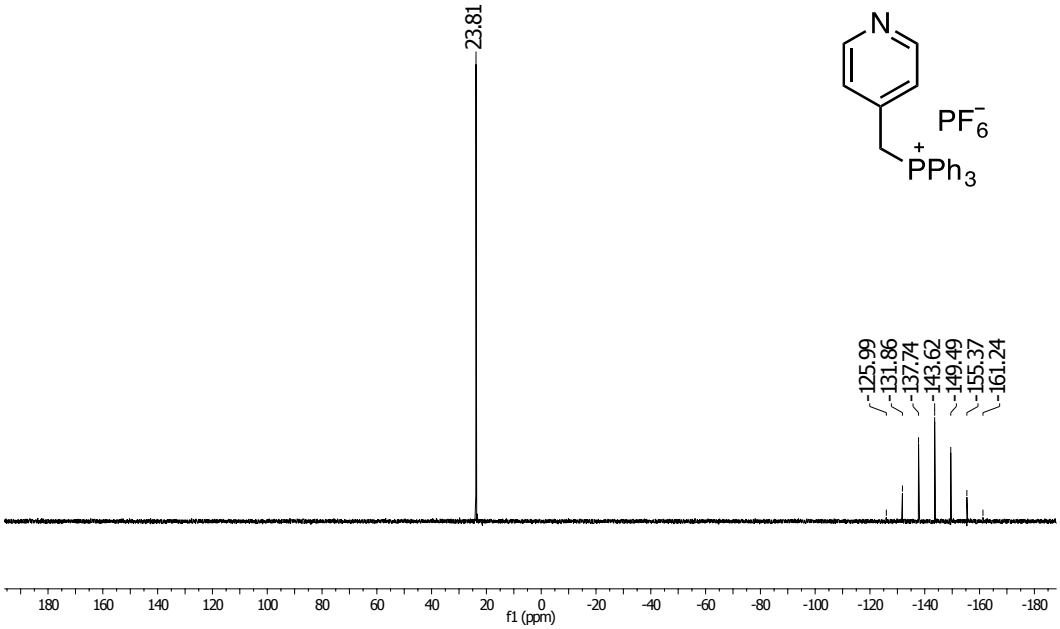

Figure S4 ^{31}P NMR of **3** in $CDCl_3$.

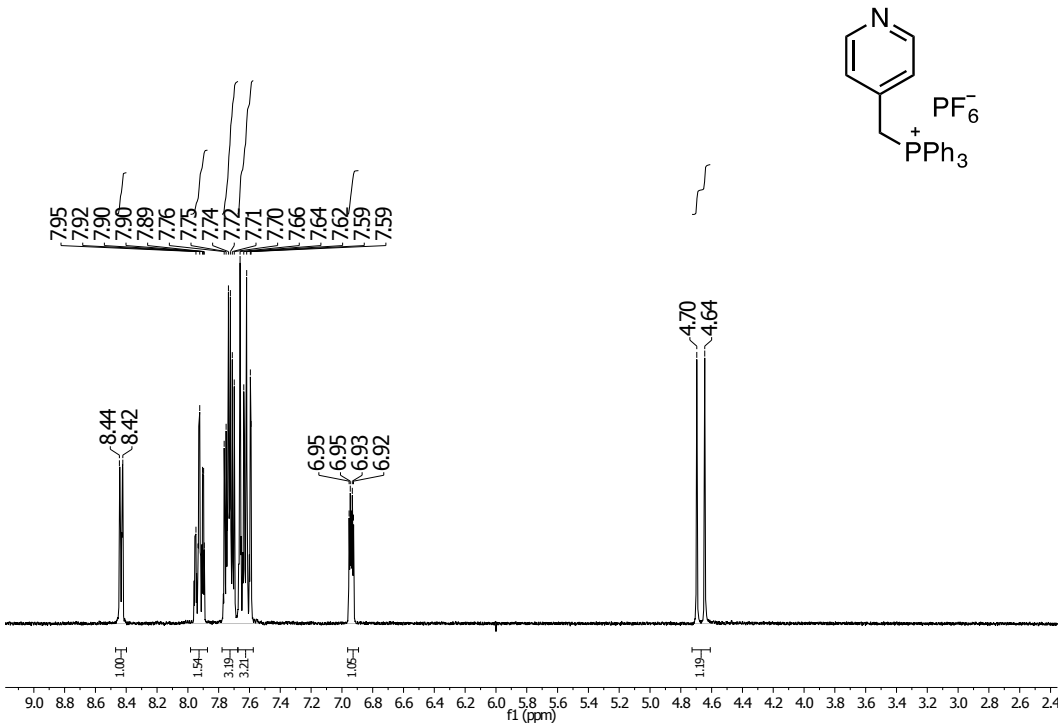

Figure S5 ^{1}H NMR of **3** in $CDCl_3$.

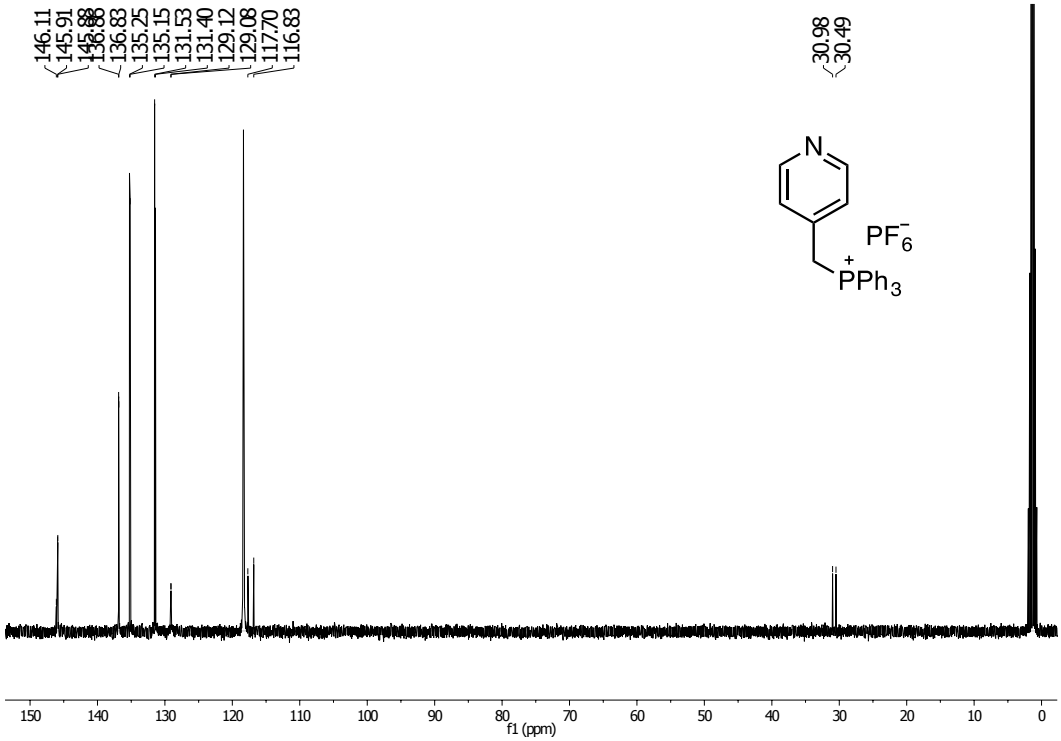

Figure S6 ^{13}C NMR of **3** in $CDCl_3$.

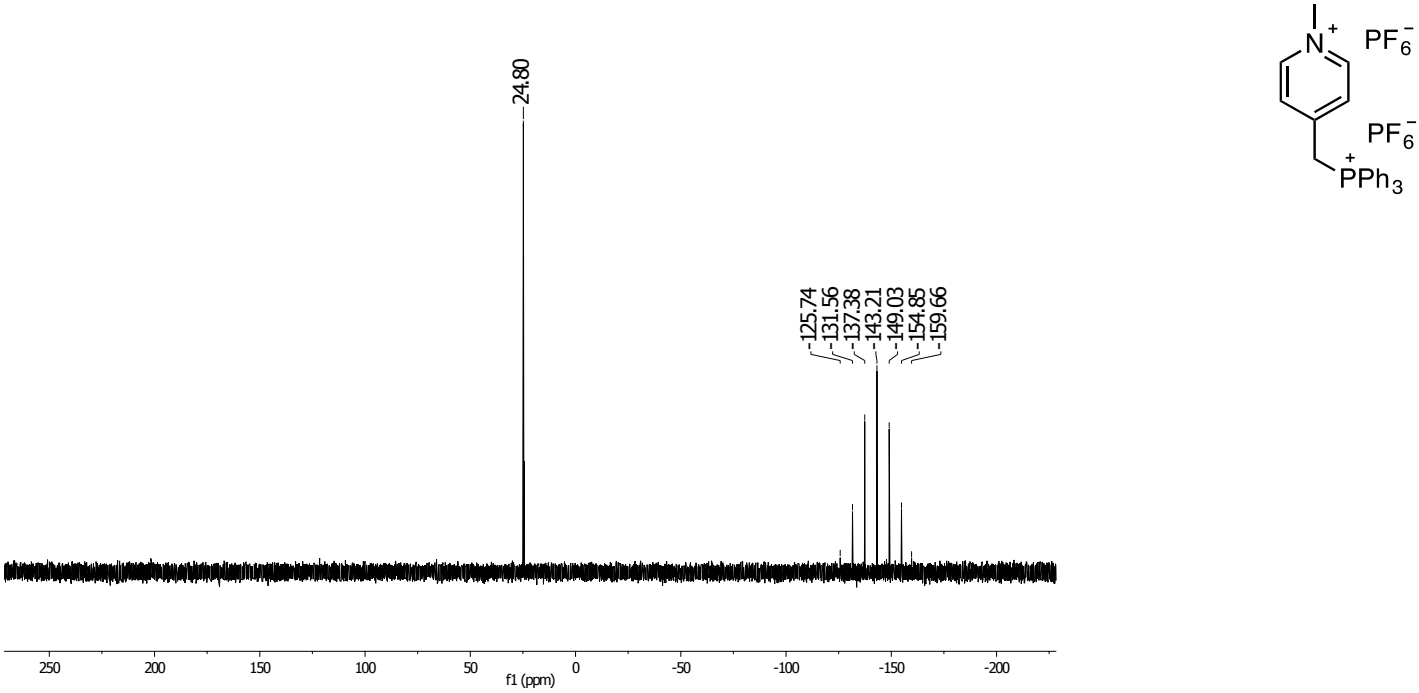

Figure S7 ^{31}P NMR of **4** in CD_3CN.

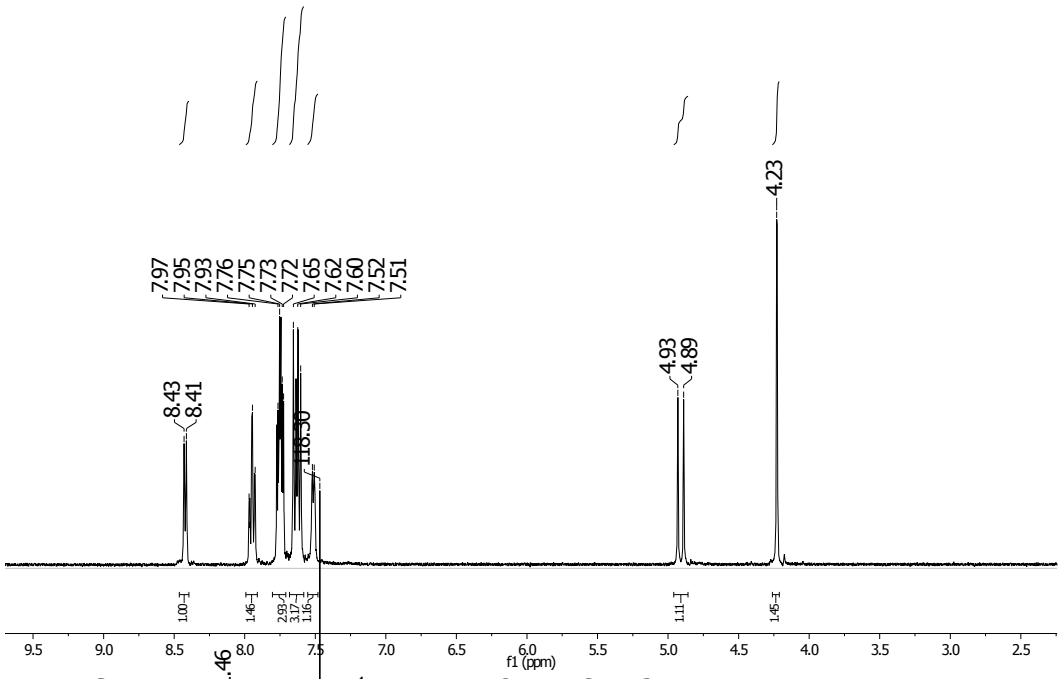

Figure S8 ^{1}H NMR of **4** in CD_3CN.

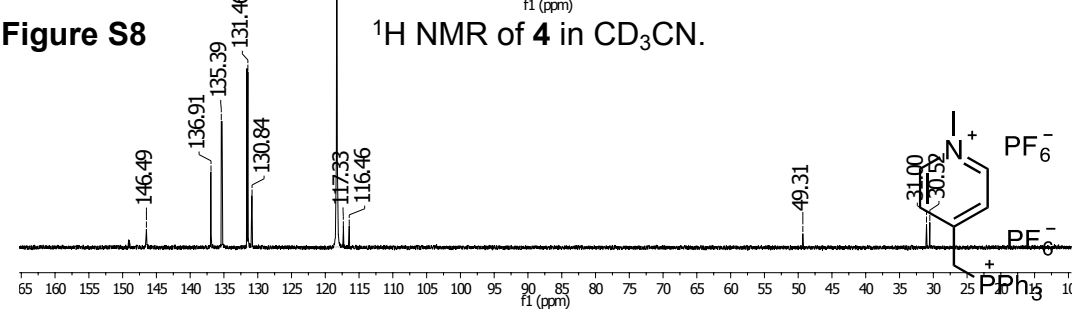

Figure S9 ^{13}C NMR of **4** in CD_3CN.

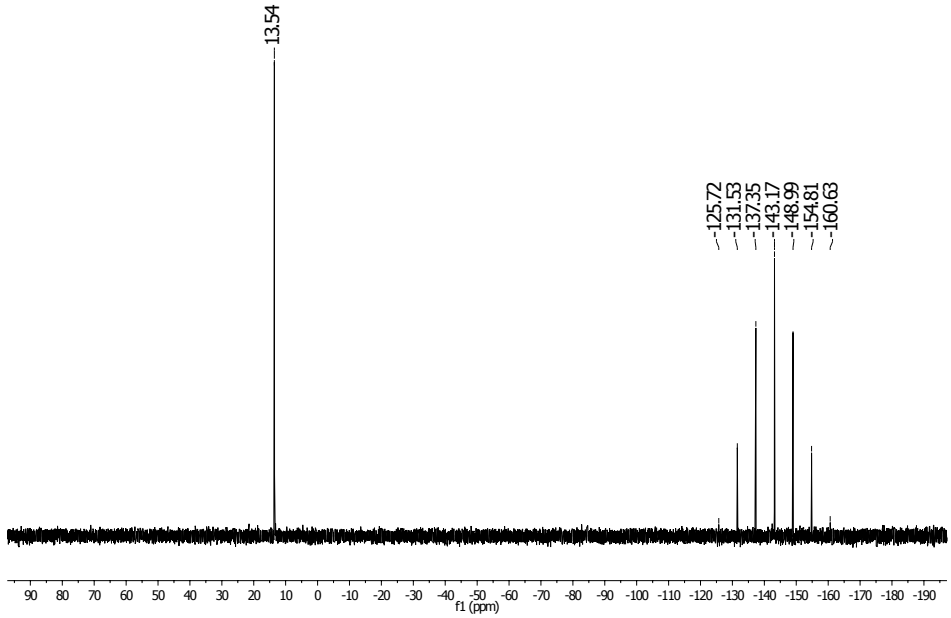

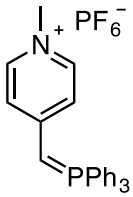

Figure S10 ^{31}P NMR of **5** in CD_3CN.

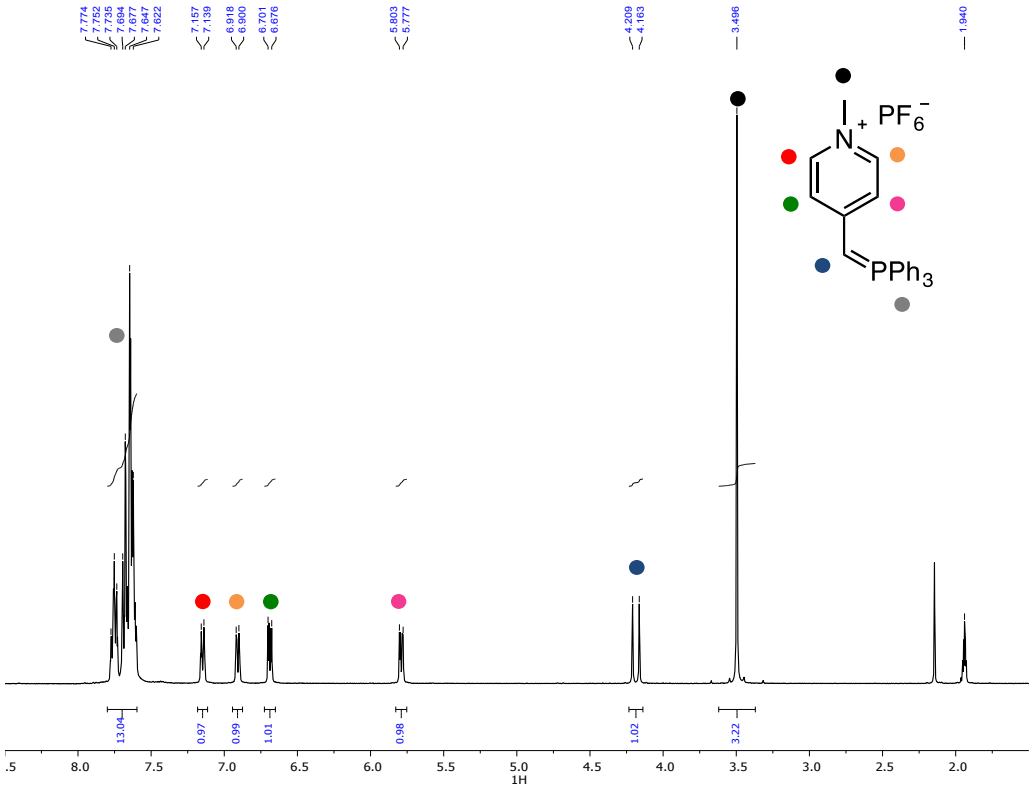

Figure S11 ^{1}H NMR of **5** in CD_3CN.

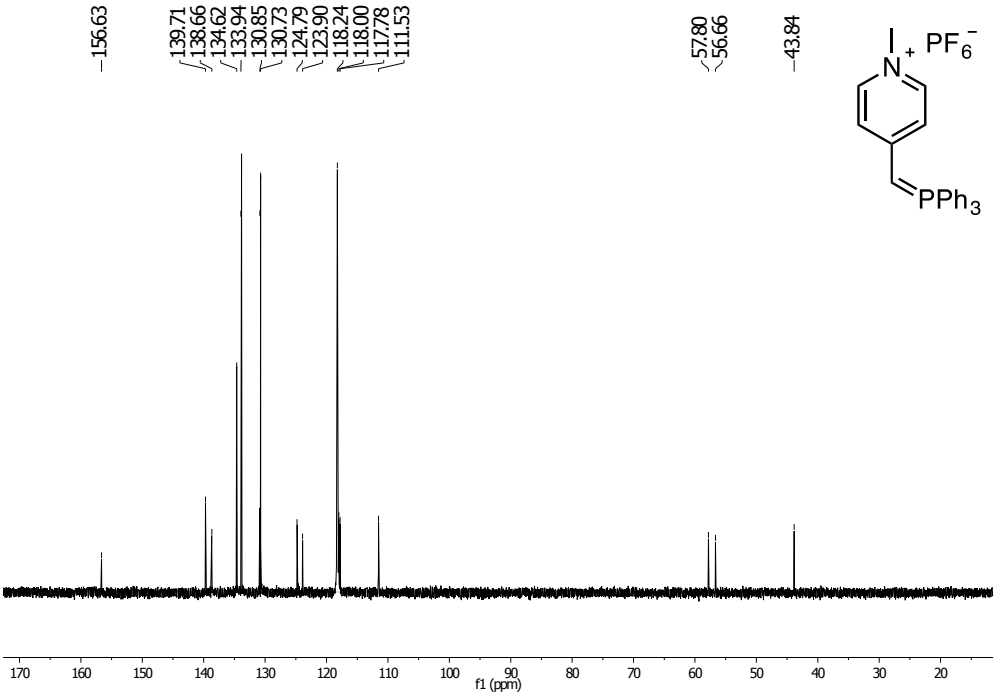

Figure S12 ^{13}C NMR of **5** in CD_3CN.

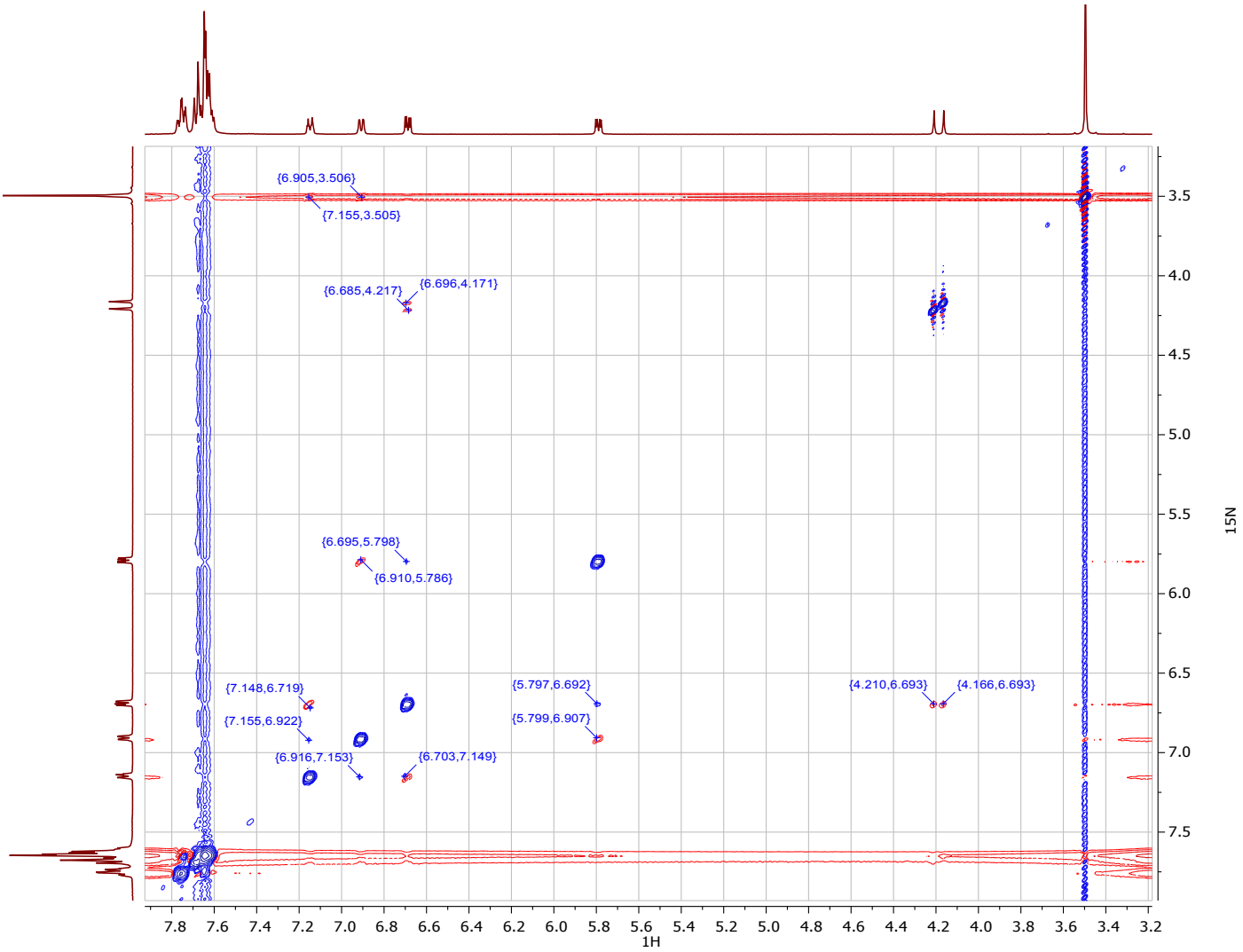

Figure S13 NOESY NMR of **5** in CD_3CN

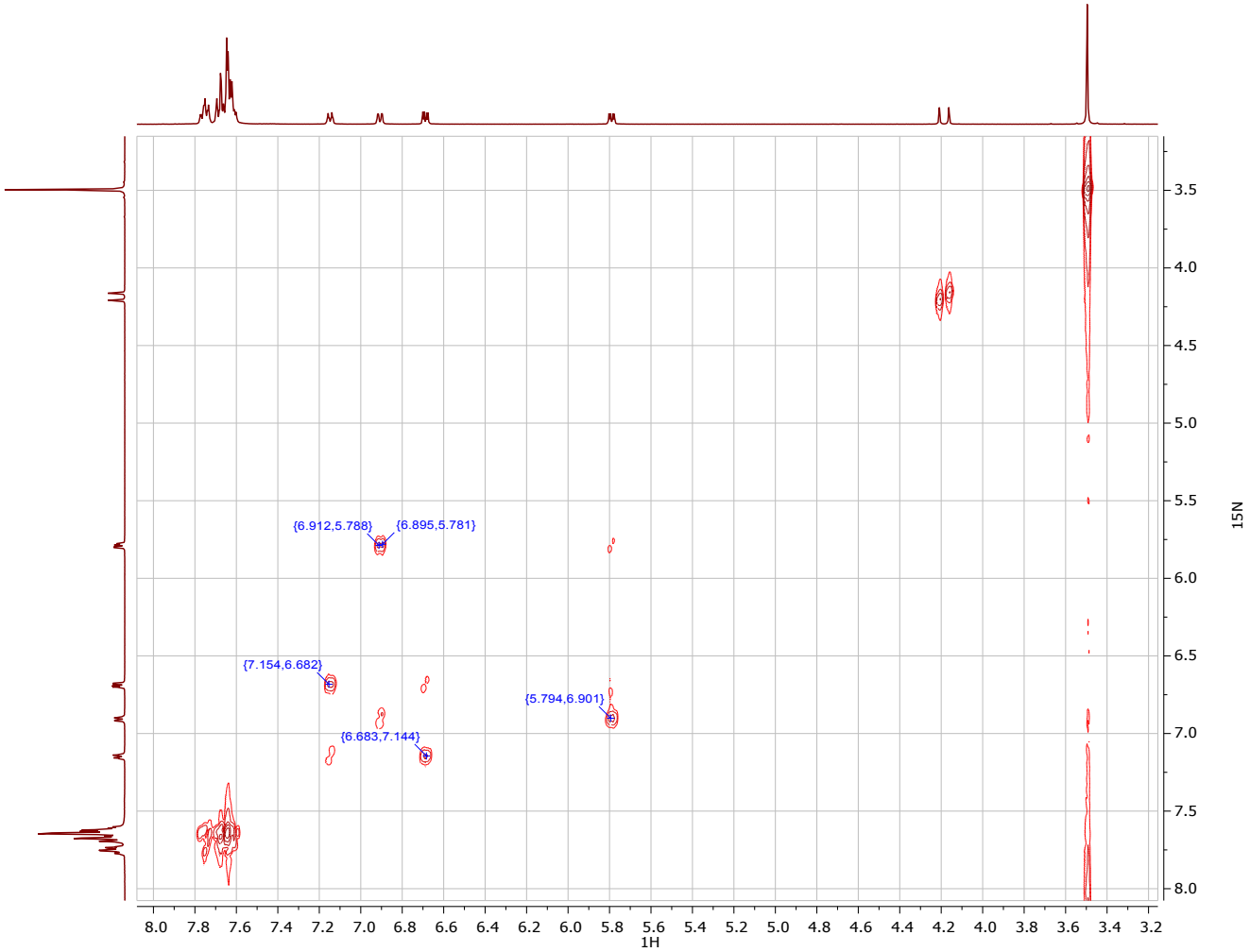

Figure S14 COSY NMR of **5** in CD_3CN

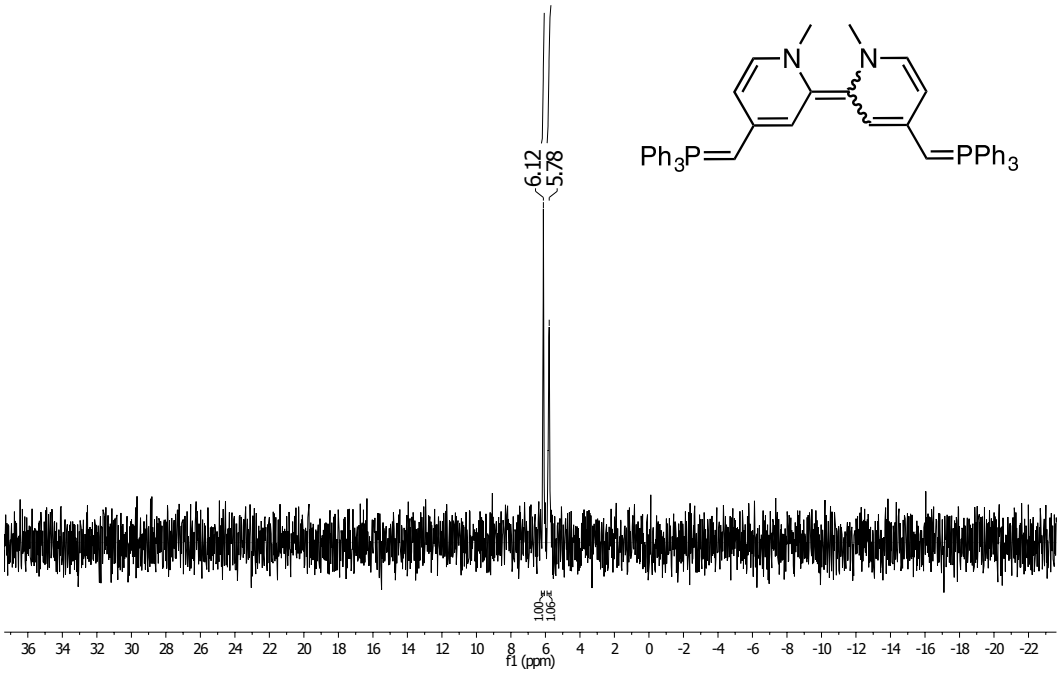

Figure S15 ^{31}P NMR of *E* and *Z* isomers of **Bd** in C_6D_6.

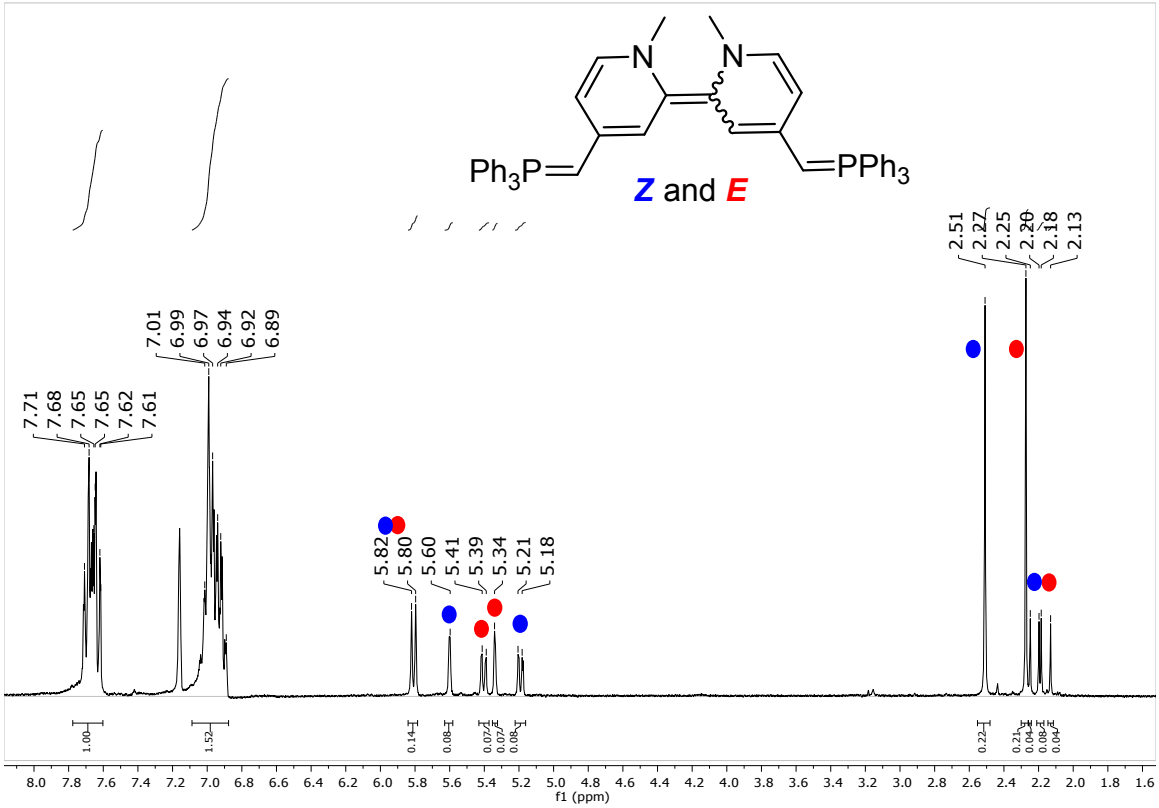

Figure S16 ^{1}H NMR of *E* and *Z* isomers of **Bd** in C_6D_6.

Figure S17 2D NOESY spectrum of *E* and *Z* isomers of **Bd** in C_6D_6. Correlations between the $CH_{pyridyl}$ and the CH_3, which defines the *E* isomer, are circled.

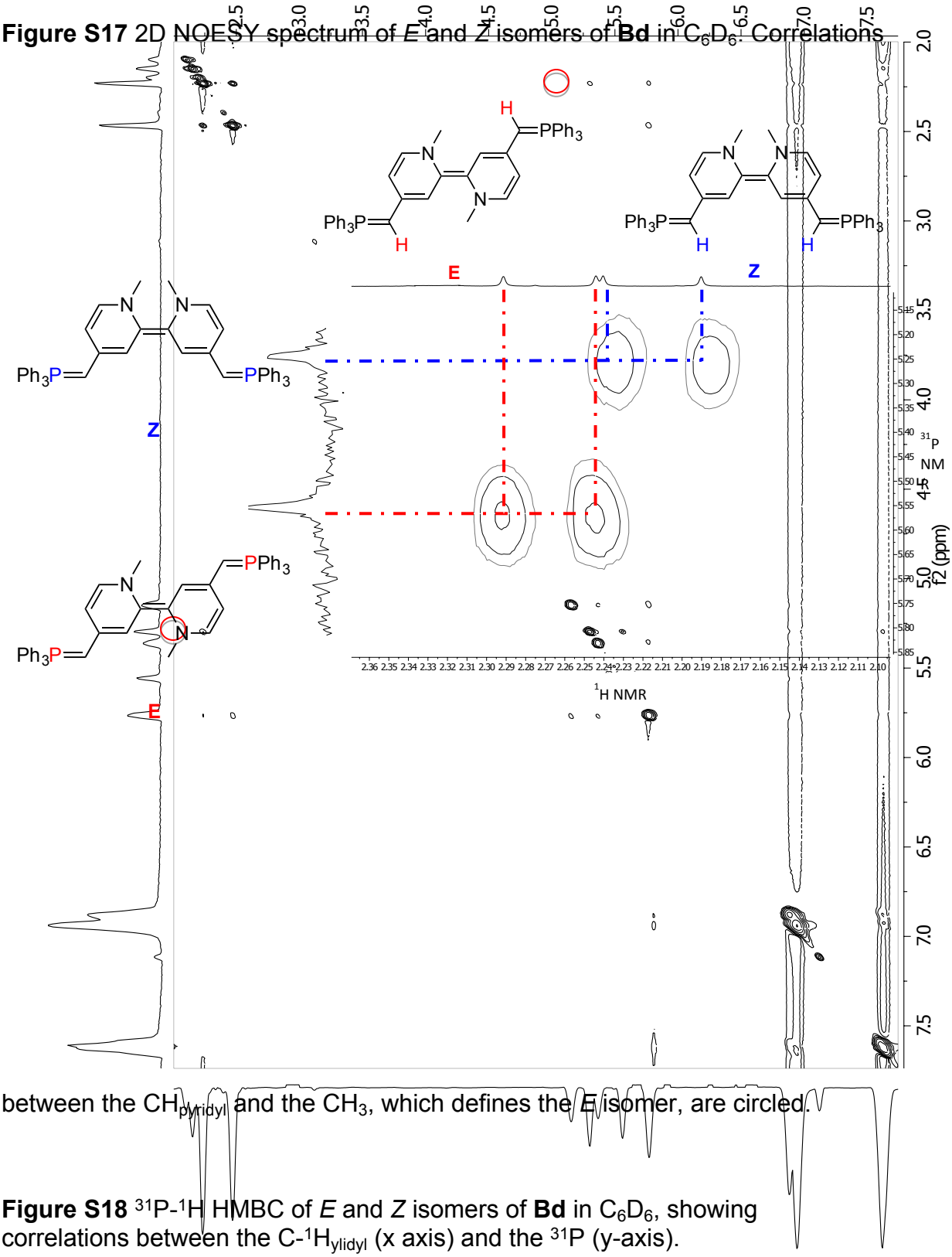

Figure S18 ^{31}P-^{1}H HMBC of *E* and *Z* isomers of **Bd** in C_6D_6, showing correlations between the C-$^{1}H_{ylidyl}$ (x axis) and the ^{31}P (y-axis).

Table 1. Selected 2D NMR correlations for isomers of Bd

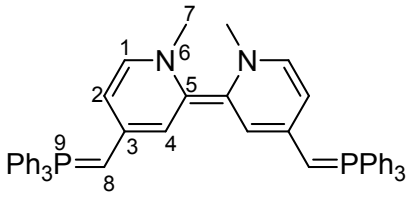

Z isomer

Atom	δ (ppm)	NOESY	^{1}H-^{31}P HMBC
1 ^{1}H	5.81	7	---
2 ^{1}H	5.19	8	---
4 ^{1}H	5.60	8	---
7 ^{1}H	2.51	1	---
8 ^{1}H	2.22	2, 4	**9**
9 ^{31}P	5.80	---	**8**

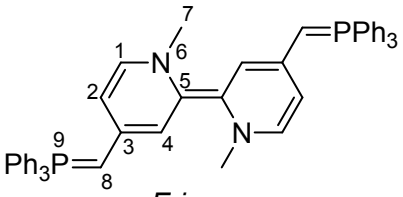

E isomer

Atom	δ (ppm)	NOESY	^{1}H-^{31}P HMBC
1 ^{1}H	5.81	7	---
2 ^{1}H	5.40	8	---
4 ^{1}H	5.34	**7**	---
7 ^{1}H	2.27	1, **4**	---
8 ^{1}H	2.17	2	**8**
9 ^{31}P	6.20	---	**9**

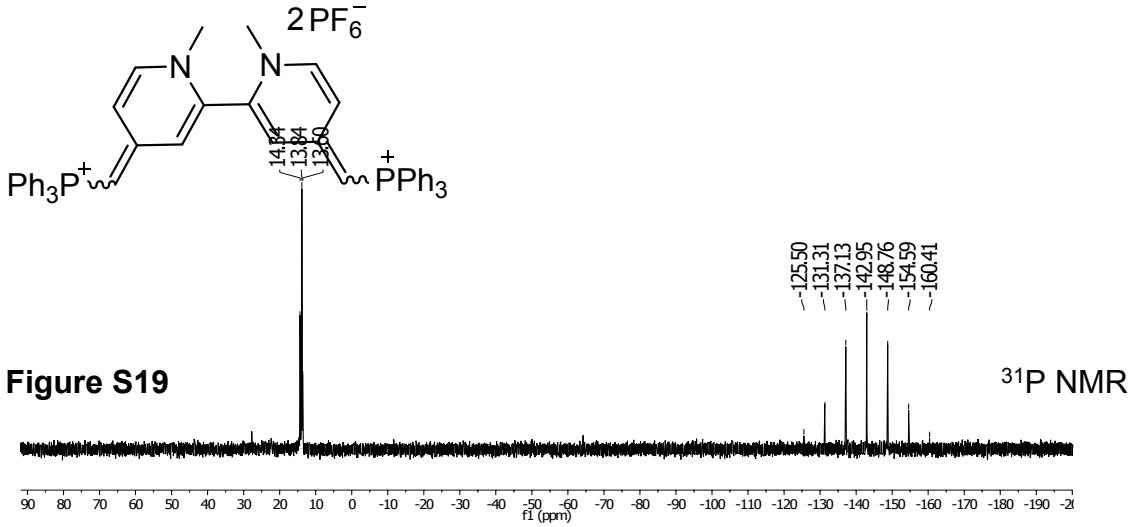

Figure S19

spectrum of mixture of **Bd^{2+}-2PF$_6^-$** in CD_3CN.

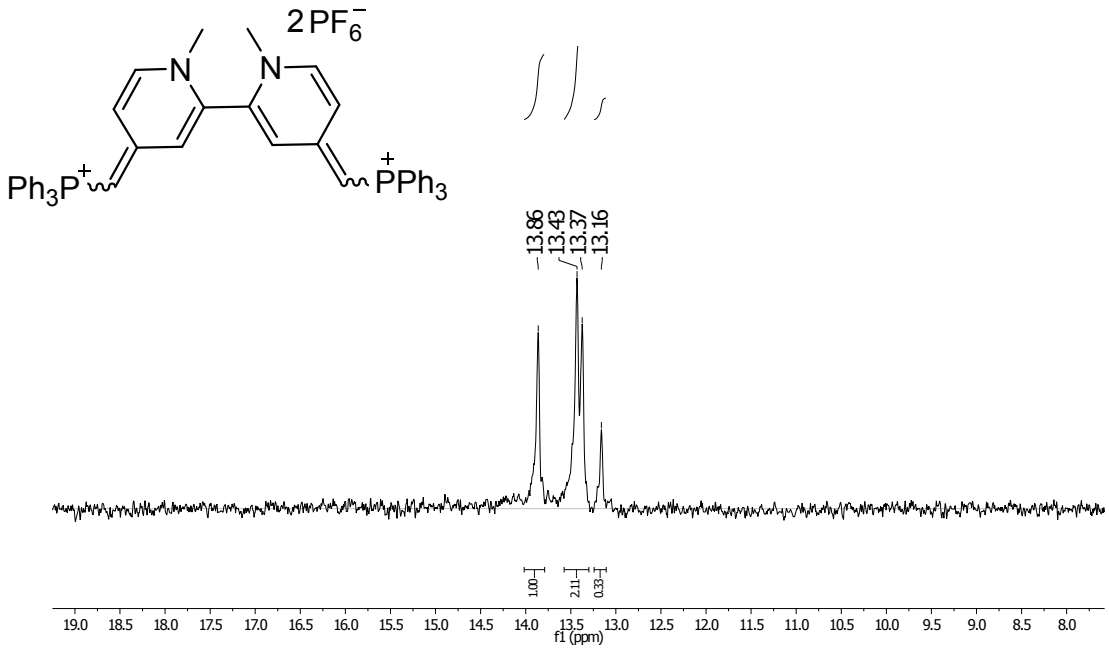

Figure S20 ^{31}P NMR of mixture of **Bd^{2+}-2PF$_6^-$** in CD_3CN (blow up of 8-19 ppm region).

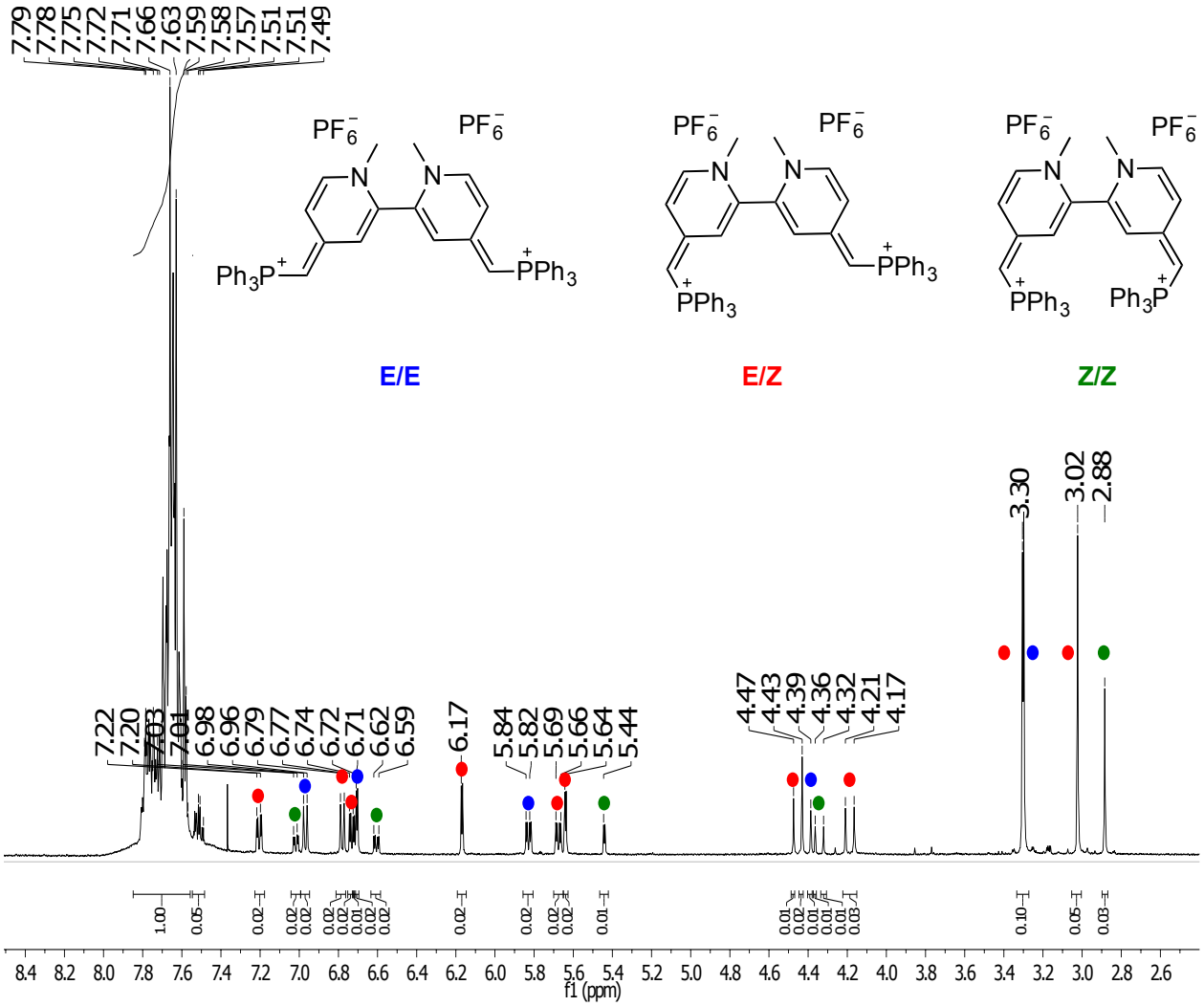

Figure S21 ^{1}H NMR of mixture of **Bd^{2+}-2PF$_6^-$** in CD_3CN.

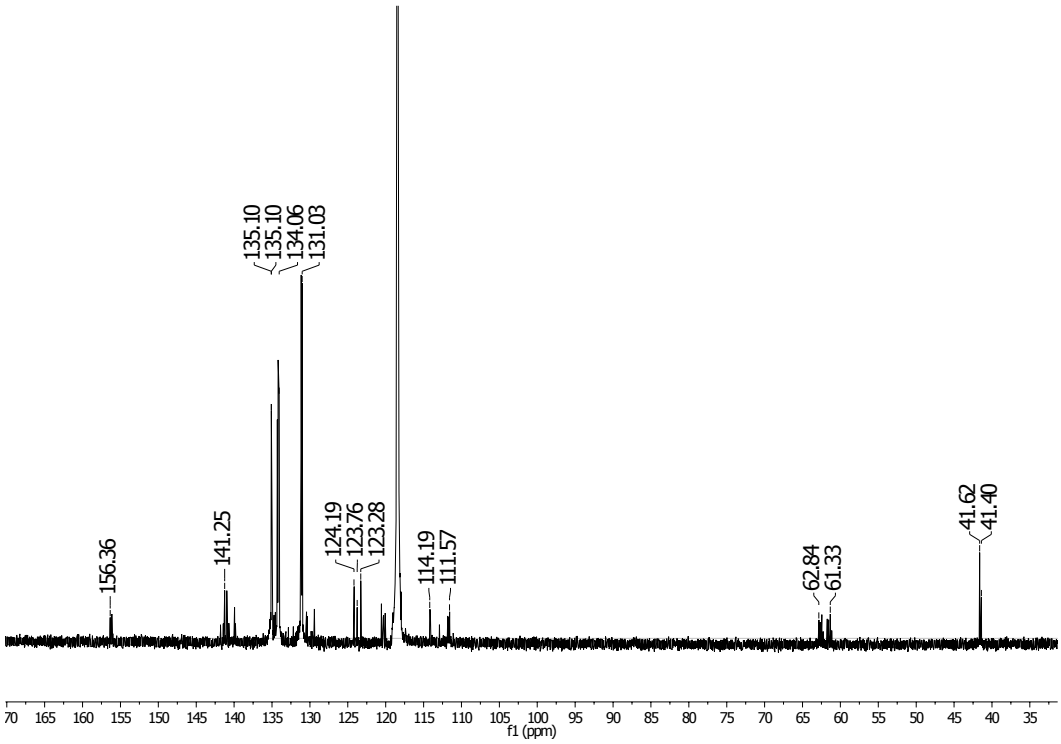

Figure S22 ^{13}C NMR of mixture of **Bd^{2+}-$2PF_6^-$** in CD_3CN.

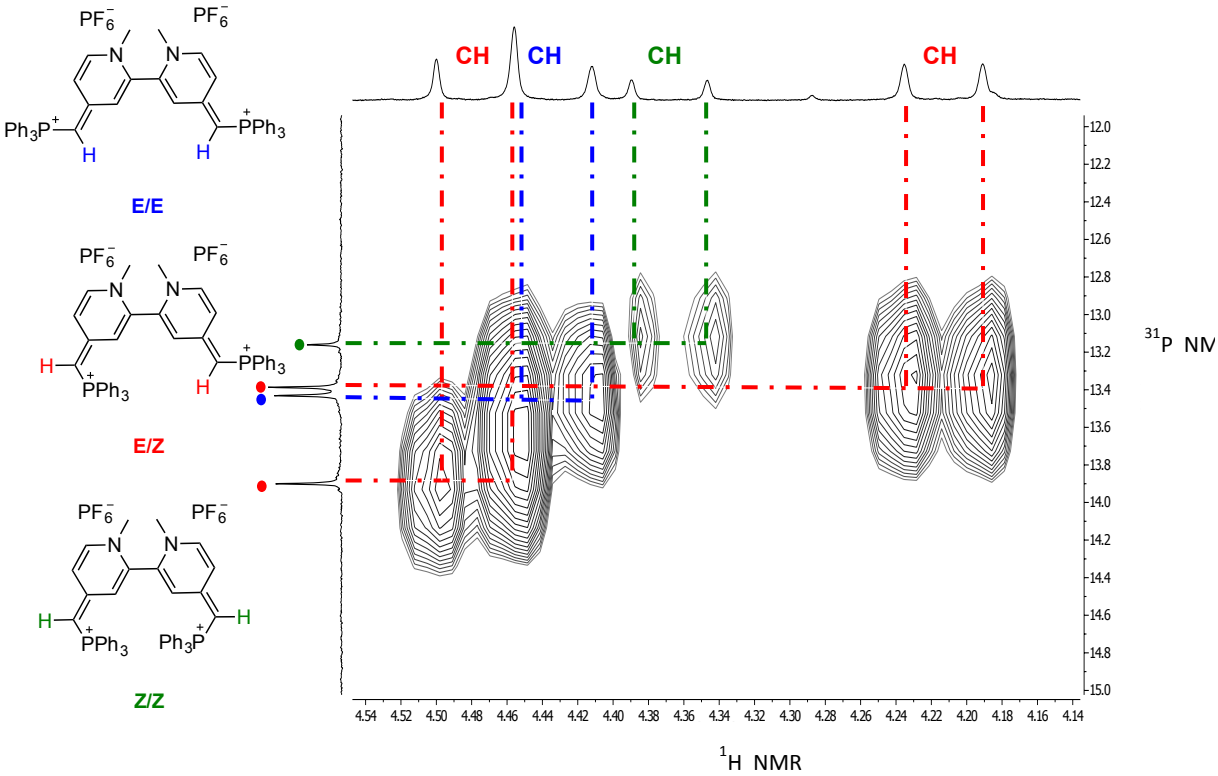

Figure S23 ^{31}P-^{1}H HMBC of mixture of **Bd^{2+}-$2PF_6^-$** in CD_3CN, showing correlations between the C-$^{1}H_{ylidyl}$ (x axis) and the ^{31}P (y-axis).

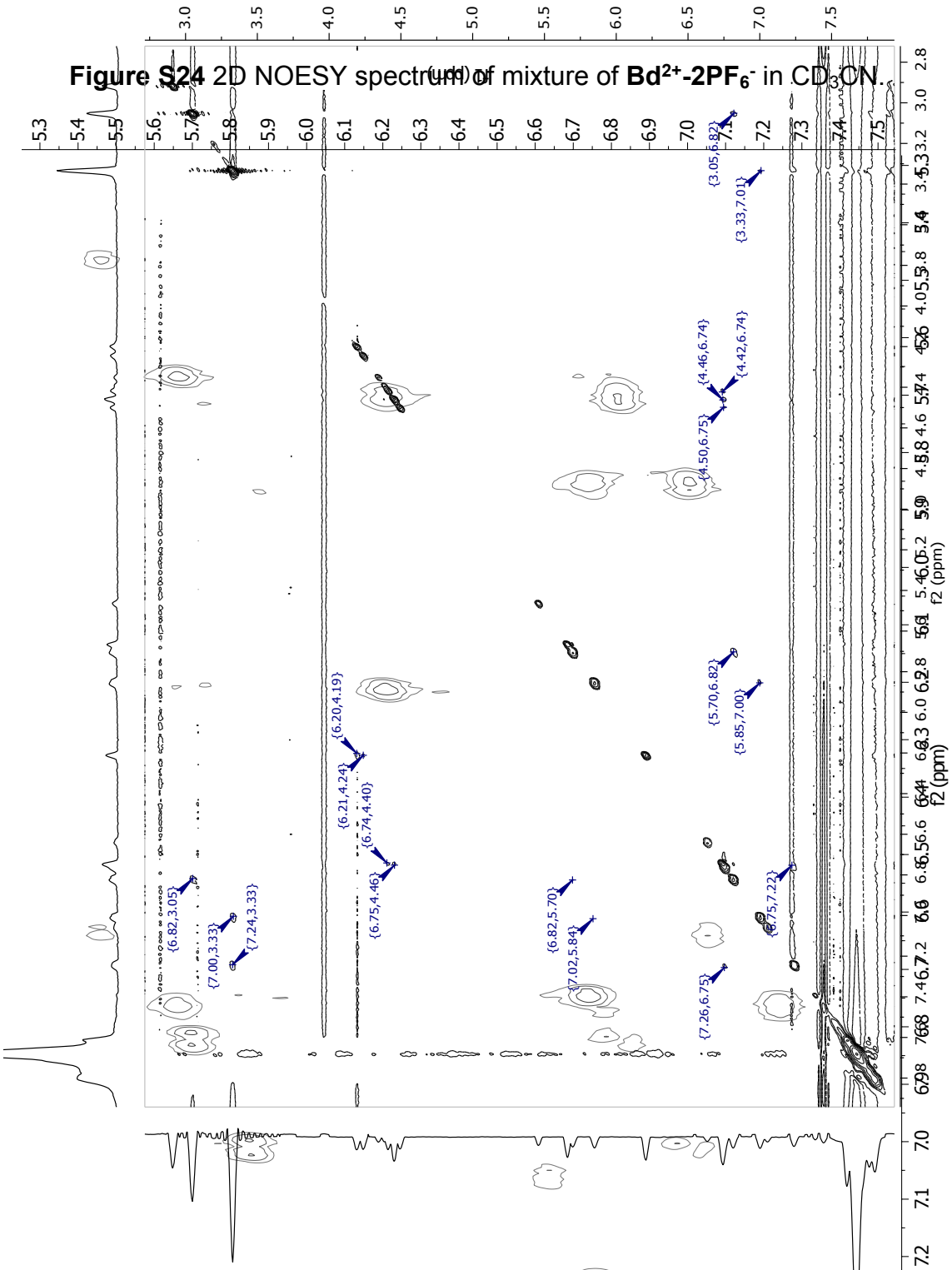

Figure S24 2D NOESY spectrum of mixture of **Bd^{2+}-2PF$_6^-$** in CD_3CN.

Figure S25 2D COSY spectrum of mixture of **Bd^{2+}-2PF$_6^-$** in CD_3CN.

Figure S26 2D ^{1}H-^{13}C NMR spectrum of mixture of **Bd^{2+}-$2PF_6^-$** in CD_3CN.

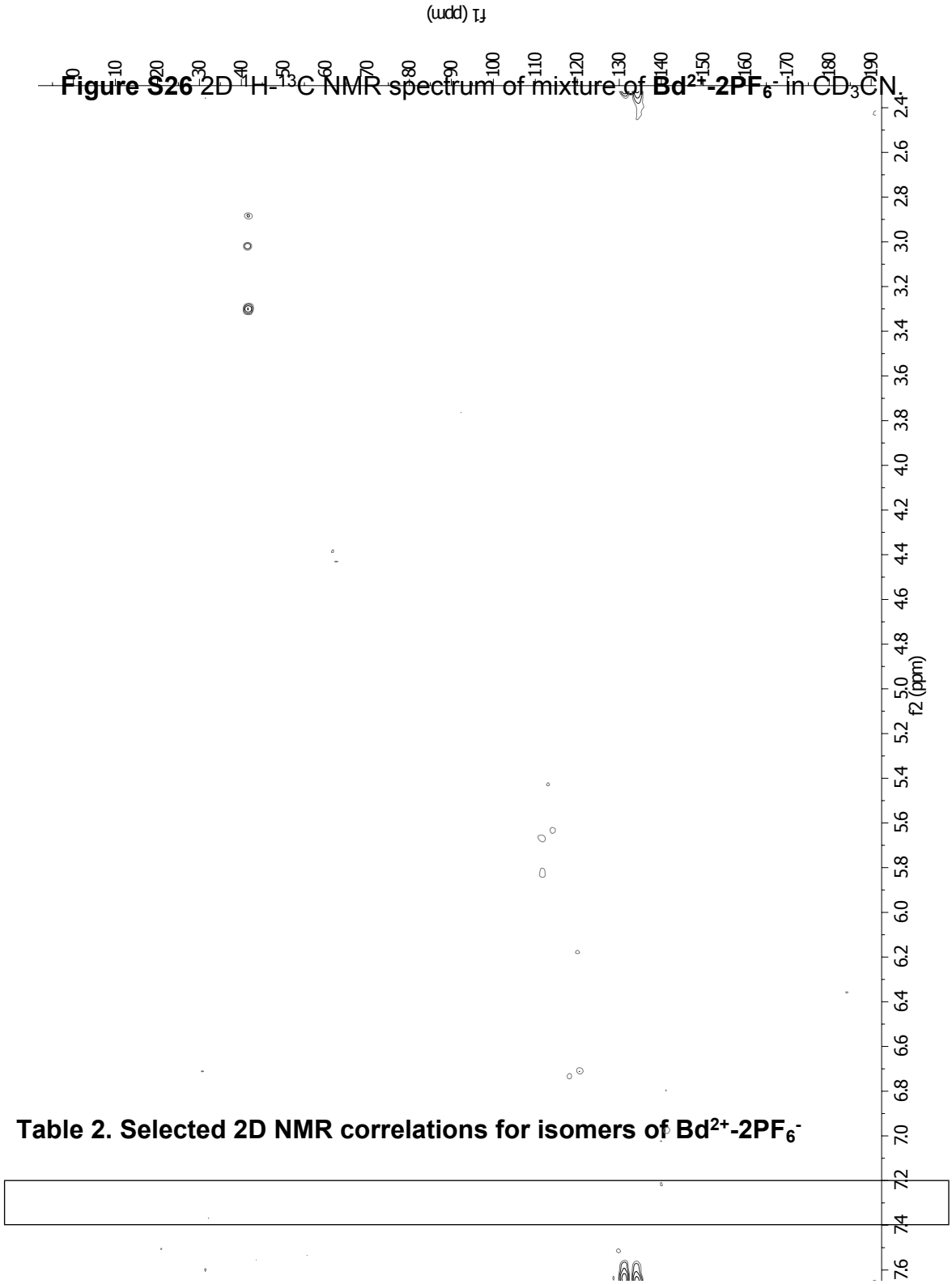

Table 2. Selected 2D NMR correlations for isomers of Bd^{2+}-$2PF_6^-$

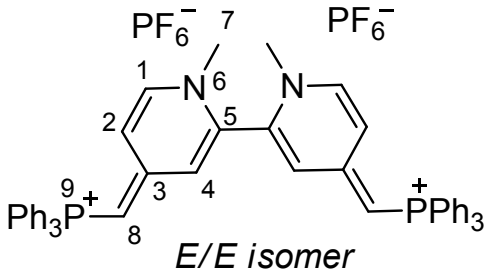

E/E isomer
32% of mixture

Atom		δ (ppm)	NOESY	COSY	^{1}H-^{31}P HMBC
1	^{1}H	7.01	2, 7	2 ($^{3}J_{HH}$= 7.5 Hz)	---
2	^{1}H	5.86	1	1 ($^{3}J_{HH}$= 7.5 Hz), 4 ($^{4}J_{HH}$= 2.7 Hz)	---
4	^{1}H	6.75	**8**	2 ($^{3}J_{HH}$= 2.7 Hz)	---
7	^{1}H	3.33	1	---	---
8	^{1}H	4.44	**4**	---	**9**
9	^{31}P	13.43	---	---	**8**

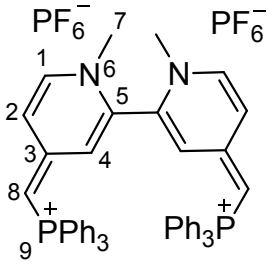

Z/Z isomer
10% of mixture

Atom		δ (ppm)	NOESY	COSY	^{1}H-^{31}P HMBC
1	^{1}H	7.06	No NOESY correlations observed for this isomer	2 ($^{3}J_{HH}$= 7.5 Hz)	---
2	^{1}H	6.64		1 ($^{3}J_{HH}$= 7.5 Hz), 4 ($^{4}J_{HH}$= 2.7 Hz)	---
4	^{1}H	5.46		2 ($^{4}J_{HH}$= 2.7 Hz)	---
7	^{1}H	2.92		---	---
8	^{1}H	4.37		---	**9**
9	^{31}P	13.16		---	**8**

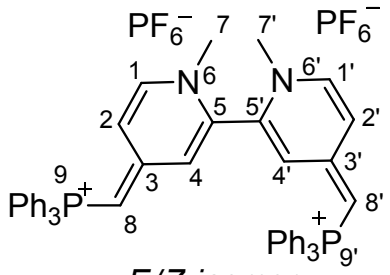

E/Z isomer
58% of mixture

Atom		δ (ppm)	NOESY	COSY	^{1}H-^{31}P HMBC
1	^{1}H	6.82	2, 7	2 ($^{3}J_{HH}$= 7.5 Hz)	---
2	^{1}H	5.71	1	1 ($^{3}J_{HH}$= 7.5 Hz), 4 ($^{4}J_{HH}$= 2.7 Hz)	---
4	^{1}H	6.20	**8**	2 ($^{4}J_{HH}$= 2.7 Hz), 4'	---
7	^{1}H	3.05	1	---	---
8	^{1}H	4.22	**4**	---	**9**
9	^{31}P	13.37	---	---	**8**
1'	^{1}H	7.25	2', 7'	2' ($^{3}J_{HH}$= 7.5 Hz)	---
2'	^{1}H	6.76	1', **8'**	1' ($^{3}J_{HH}$= 7.5 Hz), 4' ($^{4}J_{HH}$= 2.7 Hz)	---
4'	^{1}H	5.69	---	4, 2' ($^{4}J_{HH}$= 2.7 Hz)	---
7'	^{1}H	3.33	1'	---	---
8'	^{1}H	4.48	**2'**	---	**9'**
9'	^{31}P	13.86	---	---	**8'**

Cyclic Voltammagram of **Bd**

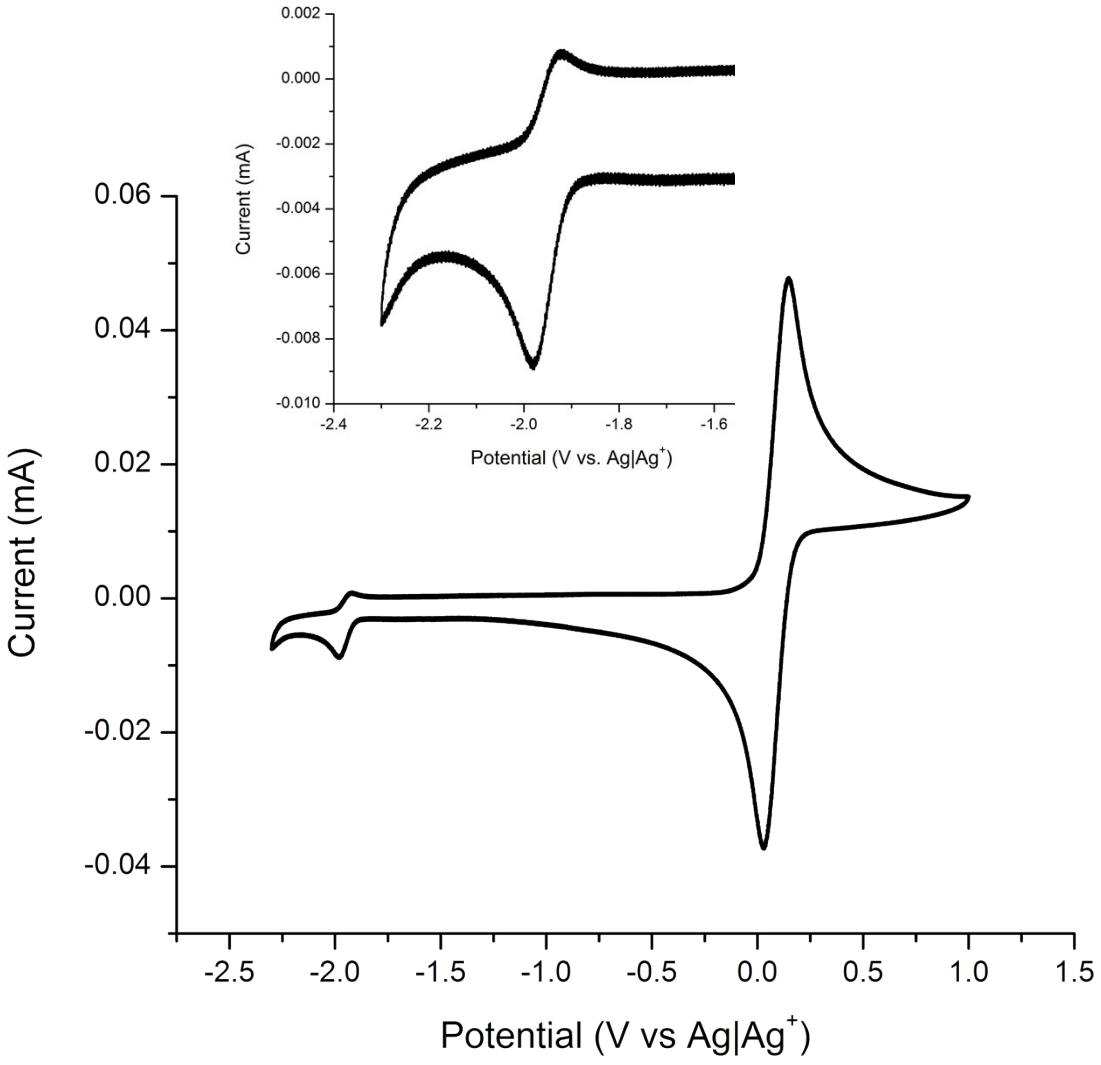

Figure S27 Cyclic voltammogram of **Bd^{2+}-$2PF_6^-$** in 0.1 M $TBAPF_6$ in DMF, with ferrocene as internal standard (scan rate of 50 mV/s). At top is a blow-up of the signal for the **Bd**/**Bd^{2+}-$2PF_6^-$** couple.

Reductions Using Bd

Reduction of Chlorodiphenylphosphine **9** to Diphosphine **10**

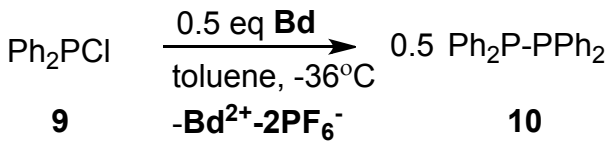

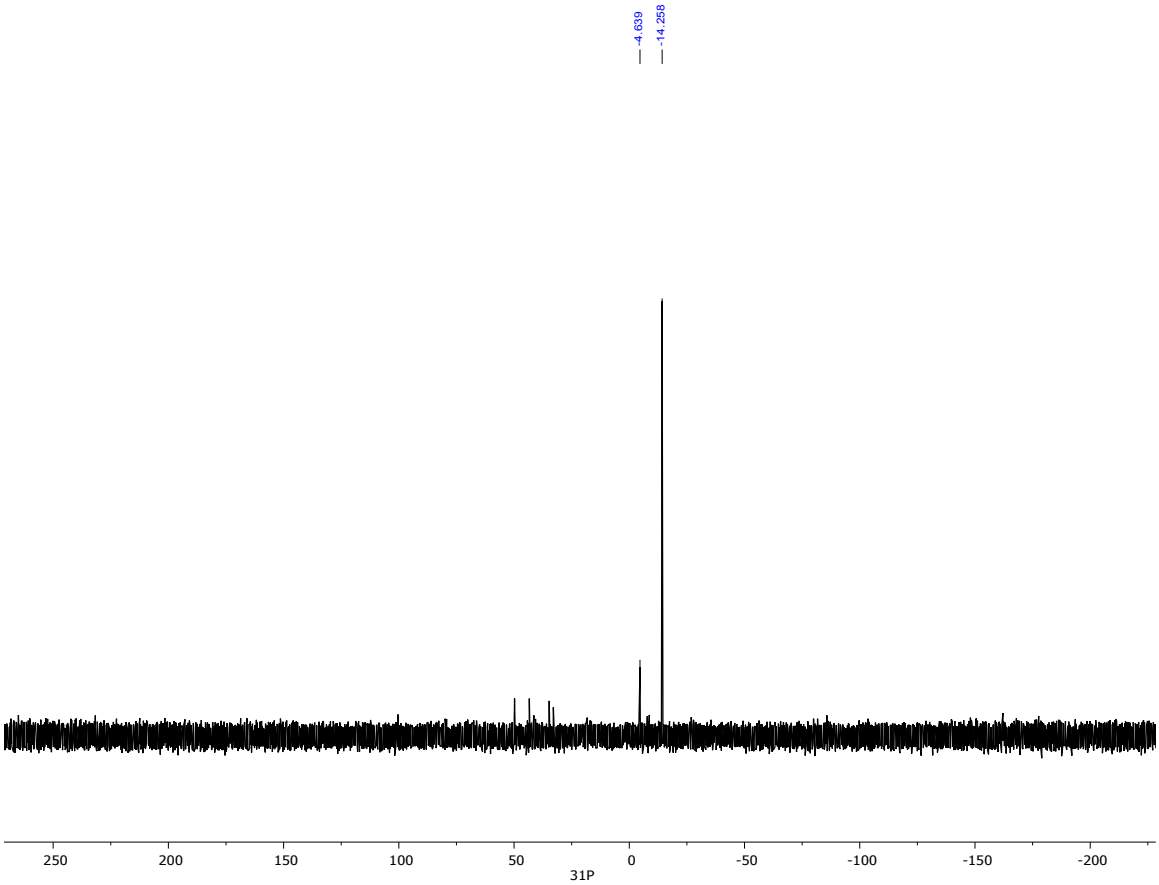

Figure S28 ^{31}P NMR spectrum of the reaction mixture of *in situ* generated **Bd** with Ph_2PCl in toluene.

Reduction of Dichlorotriphenylphosphorane **7** to Phosphine **8**

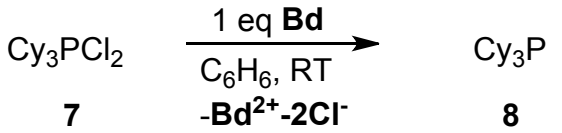

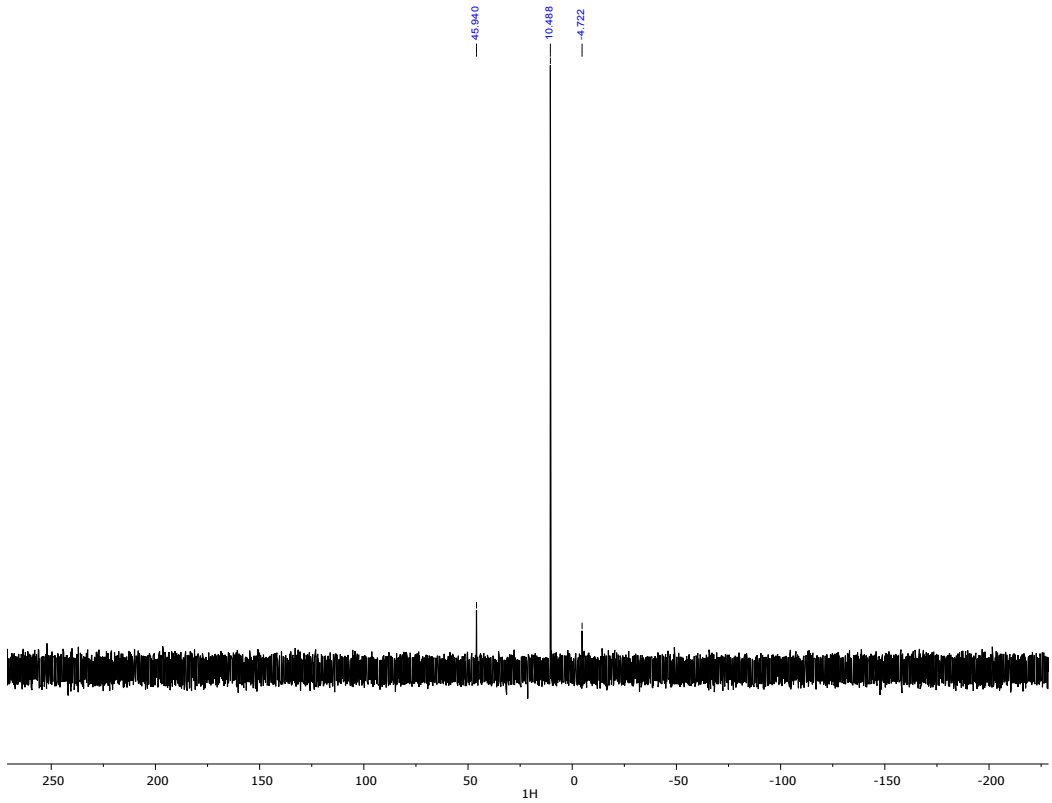

Figure S29 ^{31}P NMR spectrum of the reaction mixture of *in situ* generated **Bd** with Cy_3PCl_2 in benzene.

Variable Temperature ^{1}H NMR Inversion Transfer Experiments on 5

NMR spectra were recorded using either a Varian Inova 300 or Agilent 400 MR NMR spectrometer. Inversion transfer experiments were carried out on the 400 MR spectrometer operating under VnmrJ 3.2A using the PRESAT pulse sequence. Spectra were recorded by application of a selective 180º degree inversion pulse of 11.5 ms applied to the ^{1}H signal at 6.81 ppm, followed, after a variable delay time, by a non-selective 90º pulse. The intensities of the inverted signal at 6.81 ppm, and the exchange coupled signal at 5.70 ppm were measured using VnmrJ 4.2 software by applying a baseline correction to the spectra followed by manual selection of the integral reset points. The exchange rates at each temperature were determined by fitting the integrations of the inverted and exchange-coupled signal as a function of the variable delay time to a two-site exchange model using either Bain's CIFIT program,[1] or a spreadsheet programmed with the McConnell equations for two-site exchange as described by Led and Gesmar.[2]

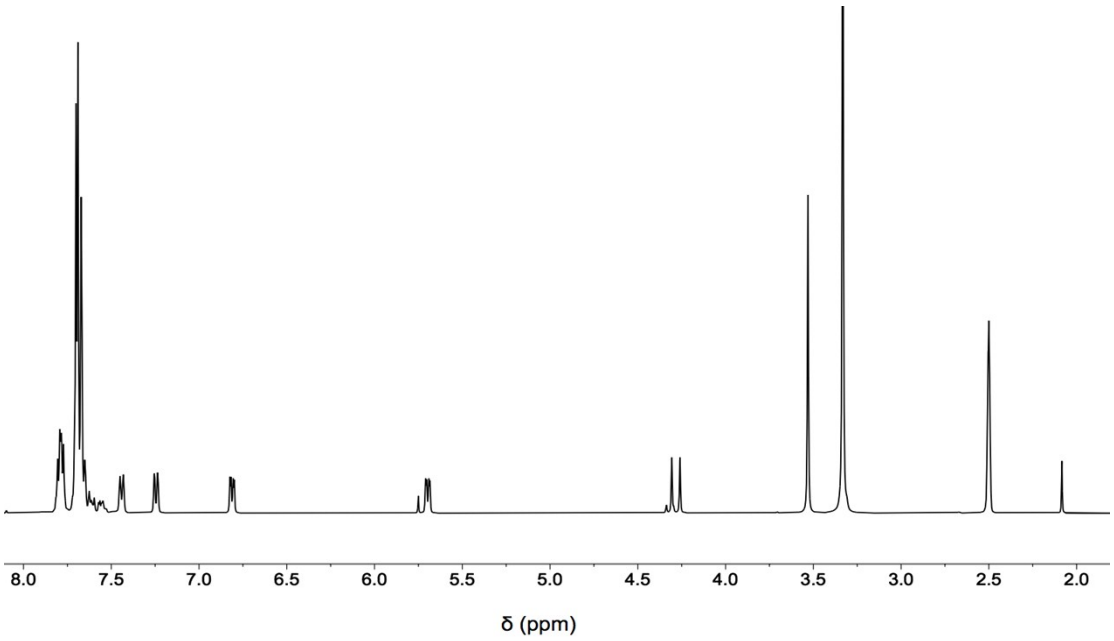

Figure S30. Expansion of the ^{1}H NMR spectrum of **5** recorded in dmso-*d*6 at 25 ºC**.**

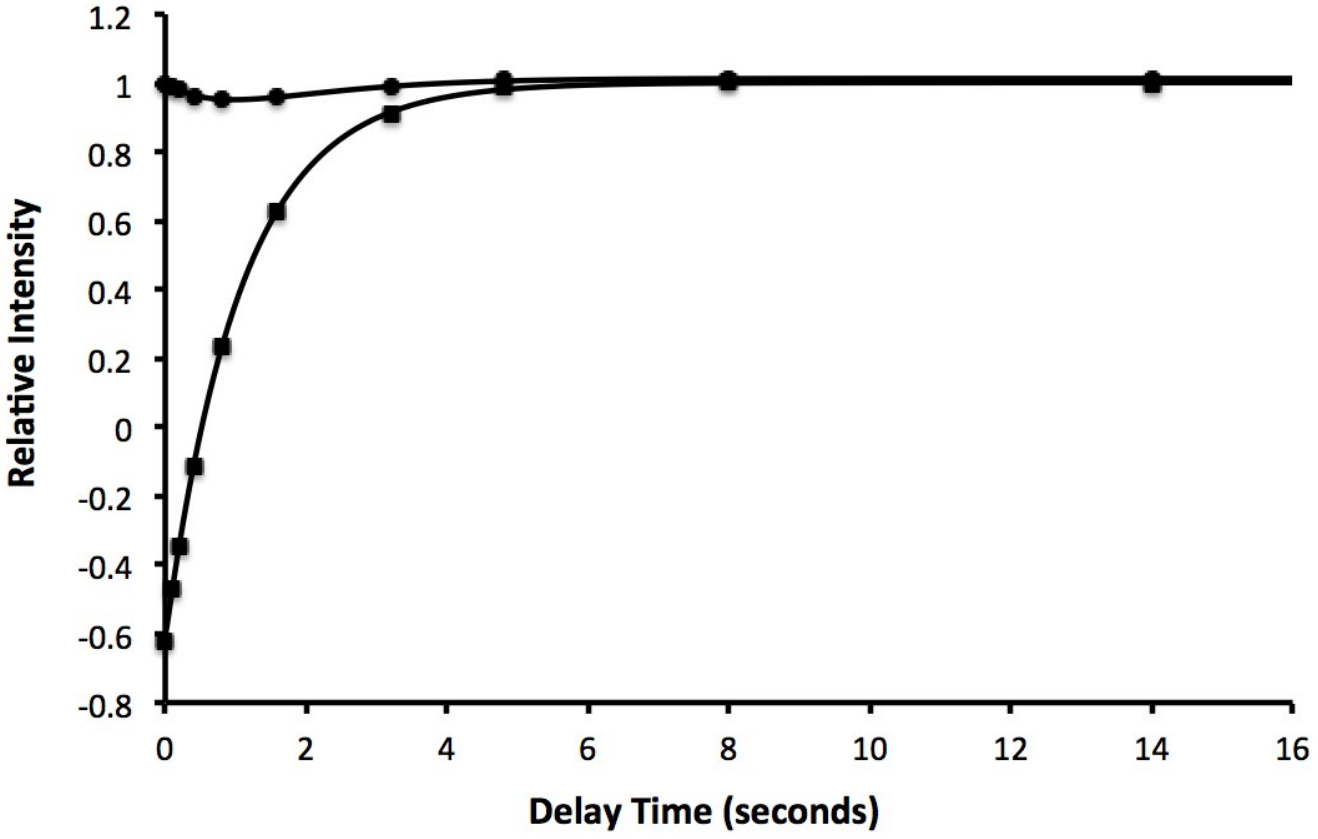

Figure S31. Results of an inversion-transfer experiment performed on 5 in dmso-*d*6 at 20 °C.

The relative intensities of the ^{1}H NMR resonances of the partially inverted signal at 6.81 ppm (squares) and the exchange coupled signal at 5.70 ppm (circles) were plotted as a function of inversion transfer delay time. Solid lines were calculated by least-squares fitting of the experimental data to the McConnell equations as described in Reference 1, yielding a rate constant of 0.09 ± 0.02 s^{-1}. The intensities of the two signals were scaled to adjust the intensity of 6.81 ppm signal to +1 at a delay time of 14 seconds, and to adjust the intensity of the 5.70 ppm signal to +1 at a delay time of 0 seconds.

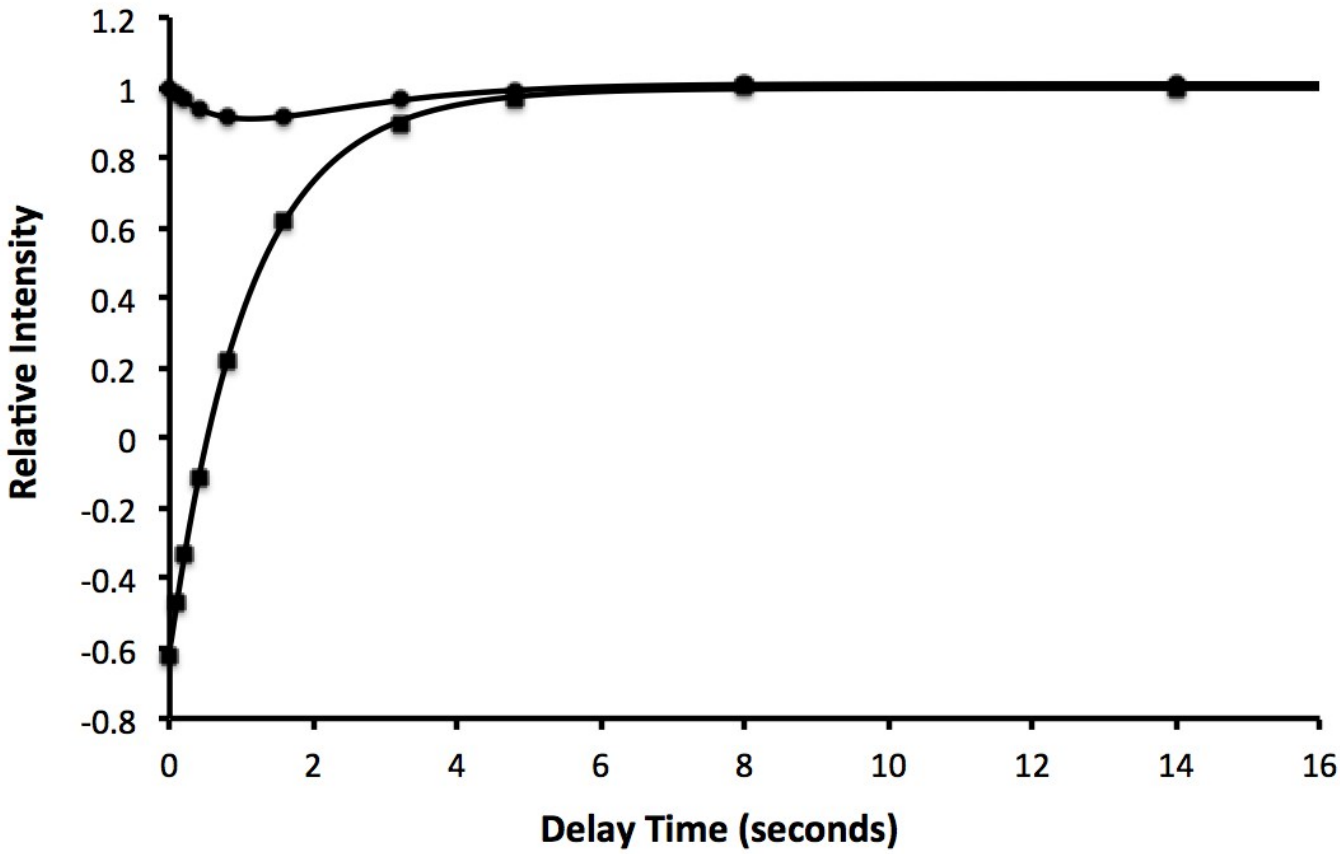

Figure S32. Results of an inversion-transfer experiment performed on 5 in dmso-*d*6 at 30 °C.

The relative intensities of the ^{1}H NMR resonances of the partially inverted signal at 6.81 ppm (squares) and the exchange coupled signal at 5.70 ppm (circles) were plotted as a function of inversion transfer delay time. Solid lines were calculated by least-squares fitting of the experimental data to the McConnell equations as described in Reference 1, yielding a rate constant of 0.14 ± 0.02 s^{-1}. The intensities of the two signals were scaled to adjust the intensity of 6.81 ppm signal to +1 at a delay time of 14 seconds, and to adjust the intensity of the 5.70 ppm signal to +1 at a delay time of 0 seconds.

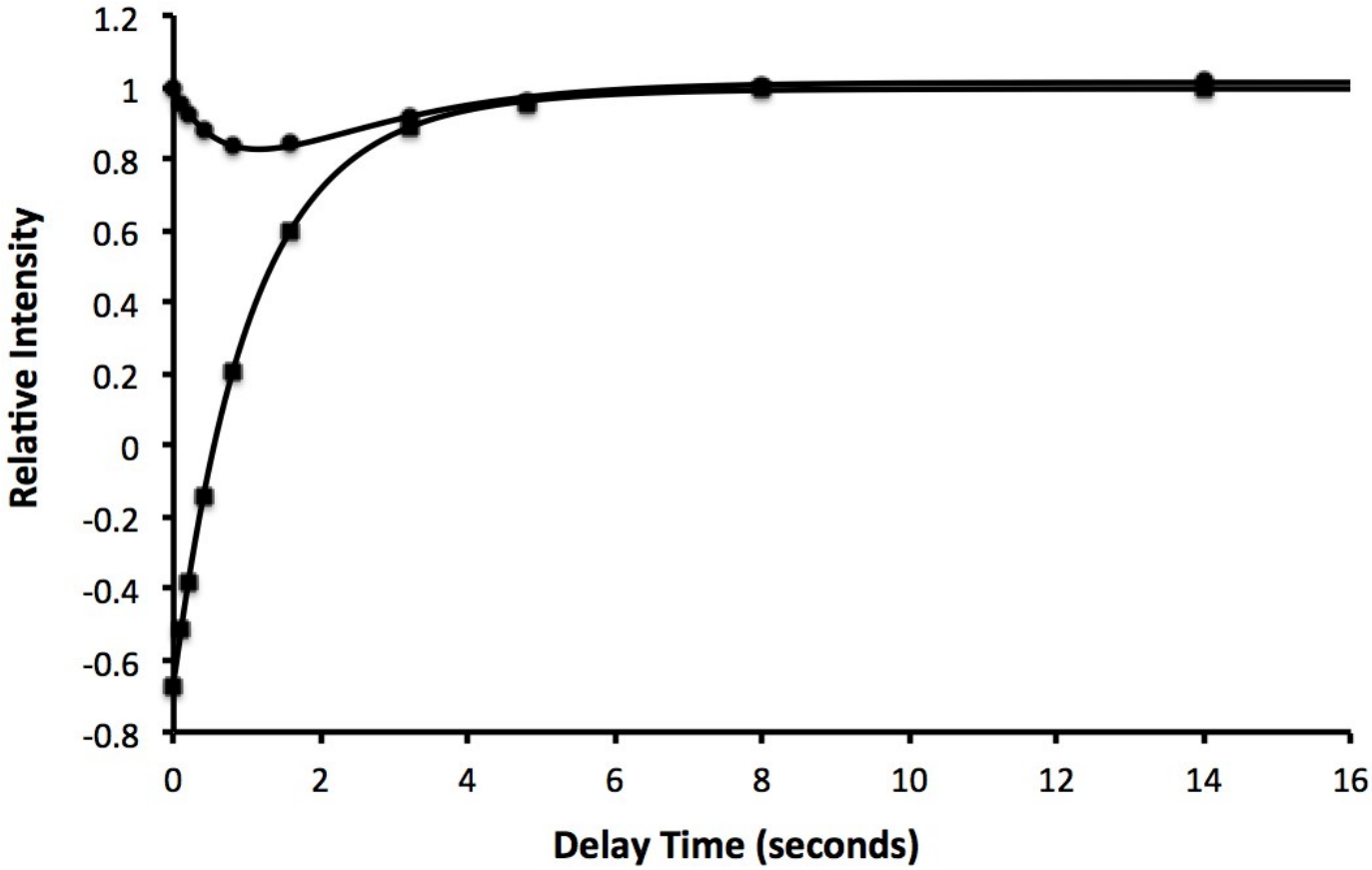

Figure S33. Results of an inversion-transfer experiment performed on 5 in dmso-*d*6 at 40 °C.

The relative intensities of the ^{1}H NMR resonances of the partially inverted signal at 6.81 ppm (squares) and the exchange coupled signal at 5.70 ppm (circles) were plotted as a function of inversion transfer delay time. Solid lines were calculated by least-squares fitting of the experimental data to the McConnell equations as described in Reference 1, yielding a rate constant of 0.23 ± 0.02 s^{-1}. The intensities of the two signals were scaled to adjust the intensity of 6.81 ppm signal to +1 at a delay time of 14 seconds, and to adjust the intensity of the 5.70 ppm signal to +1 at a delay time of 0 seconds.

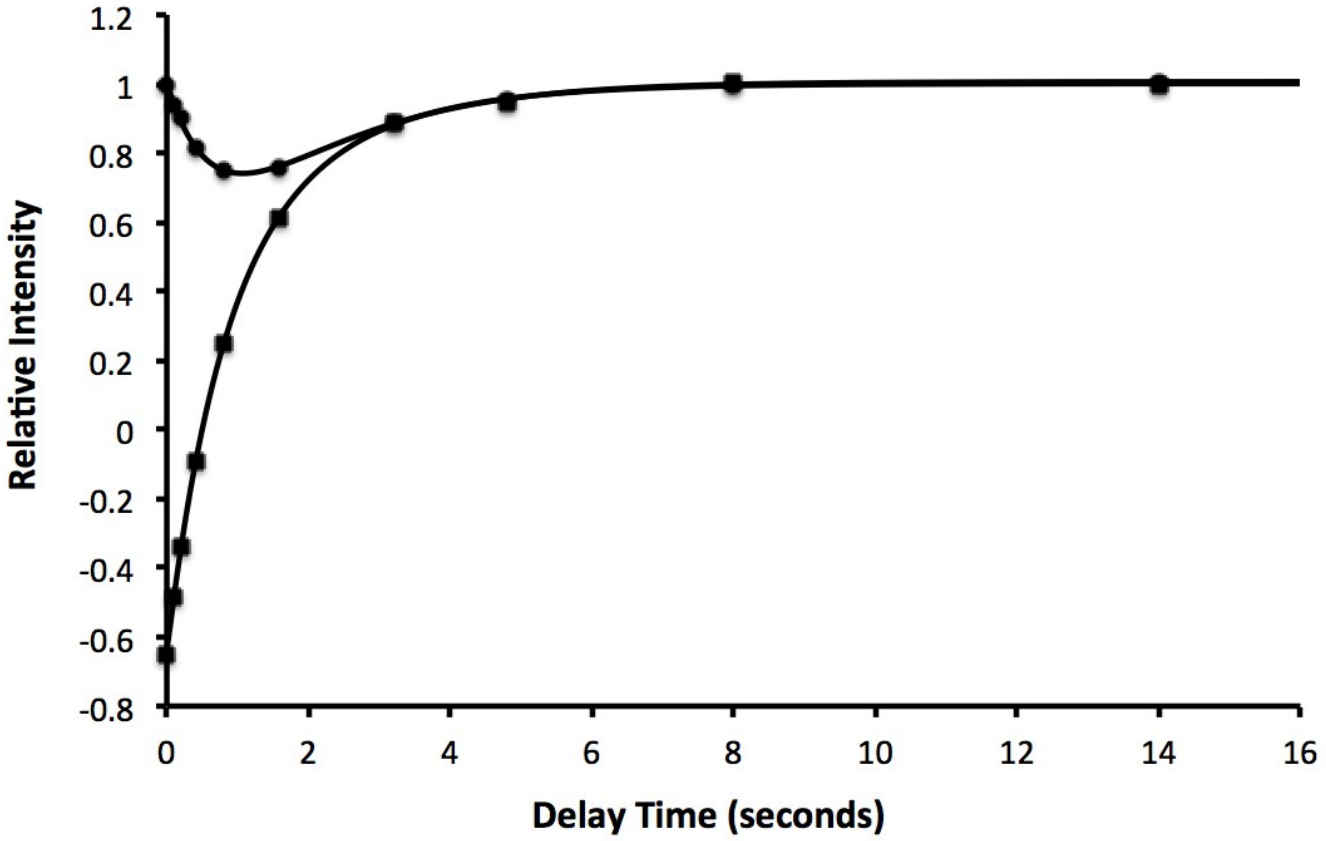

Figure S34. Results of an inversion-transfer experiment performed on 5 in dmso-*d*6 at 51 °C.

The relative intensities of the ^{1}H NMR resonances of the partially inverted signal at 6.81 ppm (squares) and the exchange coupled signal at 5.70 ppm (circles) were plotted as a function of inversion transfer delay time. Solid lines were calculated by least-squares fitting of the experimental data to the McConnell equations as described in Reference 1, yielding a rate constant of 0.40 ± 0.01 s^{-1}. The intensities of the two signals were scaled to adjust the intensity of 6.81 ppm signal to +1 at a delay time of 14 seconds, and to adjust the intensity of the 5.70 ppm signal to +1 at a delay time of 0 seconds.

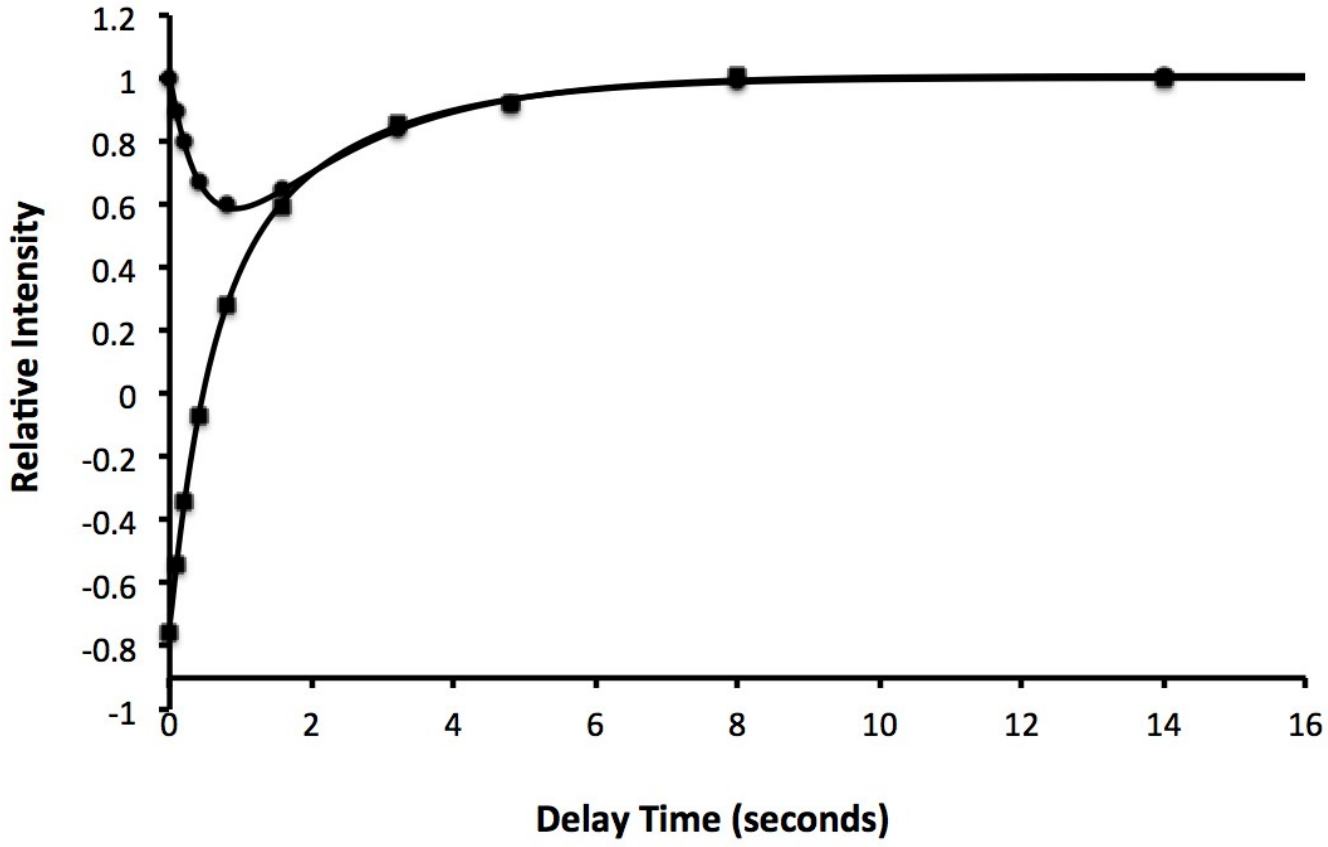

Figure S35. Results of an inversion-transfer experiment performed on 5 in dmso-*d*6 at 60 °C.

The relative intensities of the ^{1}H NMR resonances of the partially inverted signal at 6.81 ppm (squares) and the exchange coupled signal at 5.70 ppm (circles) were plotted as a function of inversion transfer delay time. Solid lines were calculated by least-squares fitting of the experimental data to the McConnell equations as described in Reference 1, yielding a rate constant of 0.74 ± 0.02 s^{-1}. The intensities of the two signals were scaled to adjust the intensity of 6.81 ppm signal to +1 at a delay time of 14 seconds, and to adjust the intensity of the 5.70 ppm signal to +1 at a delay time of 0 seconds.

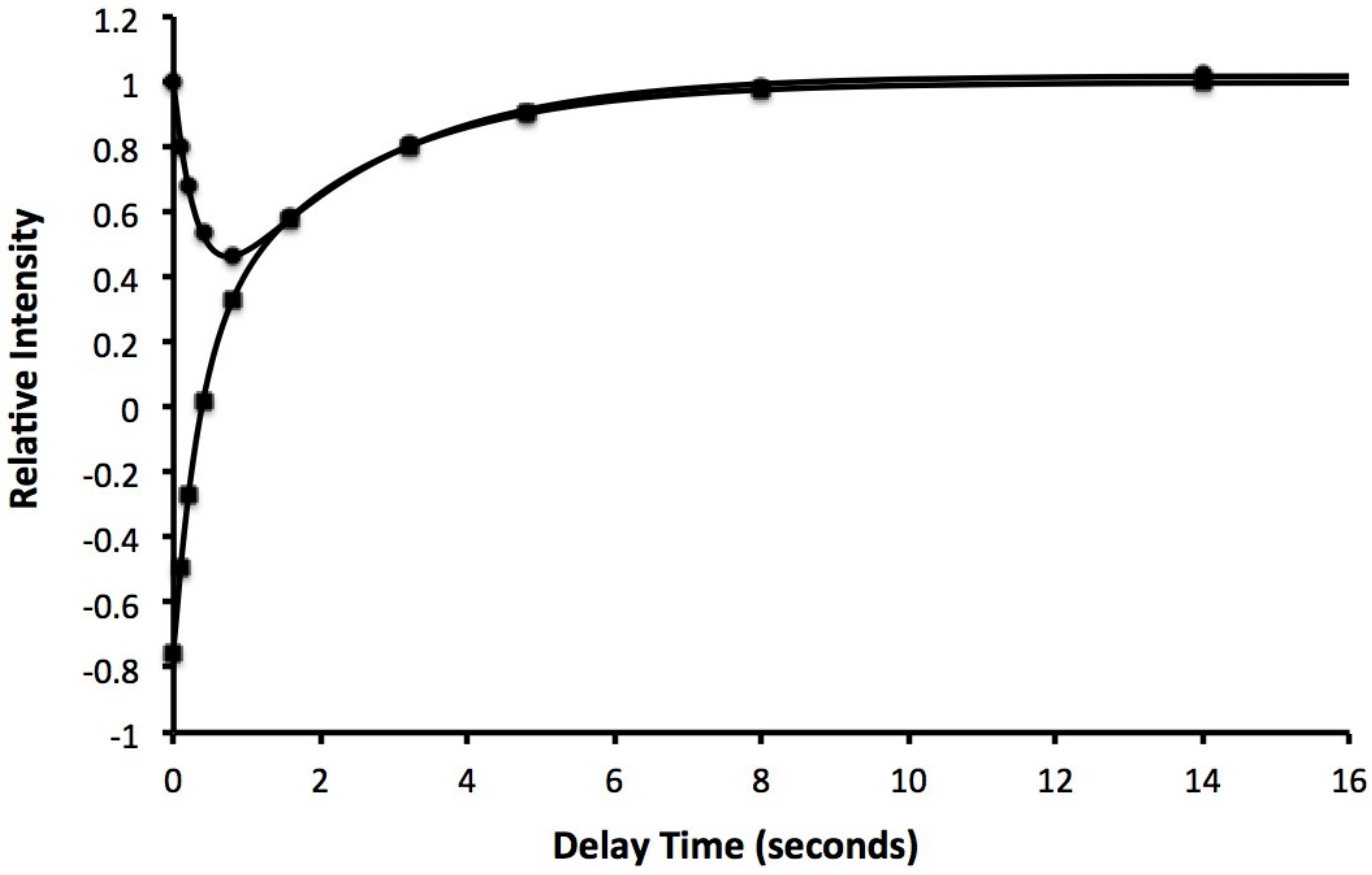

Figure S36. Results of an inversion-transfer experiment performed on 5 in dmso-*d*6 at 69 °C.

The relative intensities of the ^{1}H NMR resonances of the partially inverted signal at 6.81 ppm (squares) and the exchange coupled signal at 5.70 ppm (circles) were plotted as a function of inversion transfer delay time. Solid lines were calculated by least-squares fitting of the experimental data to the McConnell equations as described in Reference 1, yielding a rate constant of 1.26 ± 0.02 s^{-1}. The intensities of the two signals were scaled to adjust the intensity of 6.81 ppm signal to +1 at a delay time of 14 seconds, and to adjust the intensity of the 5.70 ppm signal to +1 at a delay time of 0 seconds.

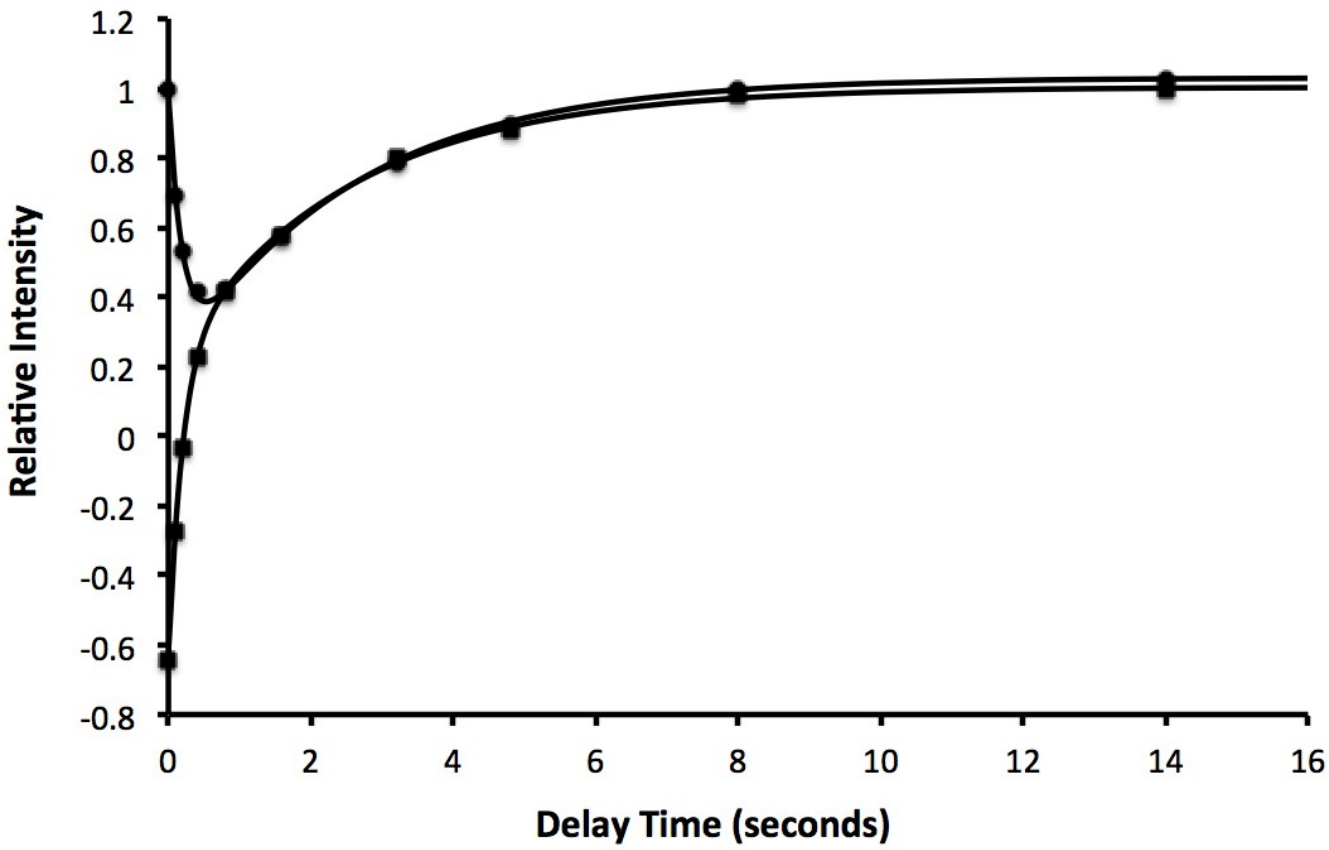

Figure S37. Results of an inversion-transfer experiment performed on 5 in dmso-*d*6 at 79 °C.

The relative intensities of the ^{1}H NMR resonances of the partially inverted signal at 6.81 ppm (squares) and the exchange coupled signal at 5.70 ppm (circles) were plotted as a function of inversion transfer delay time. Solid lines were calculated by least-squares fitting of the experimental data to the McConnell equations as described in Reference 1, yielding a rate constant of 2.39 ± 0.03 s^{-1}. The intensities of the two signals were scaled to adjust the intensity of 6.81 ppm signal to +1 at a delay time of 14 seconds, and to adjust the intensity of the 5.70 ppm signal to +1 at a delay time of 0 seconds.

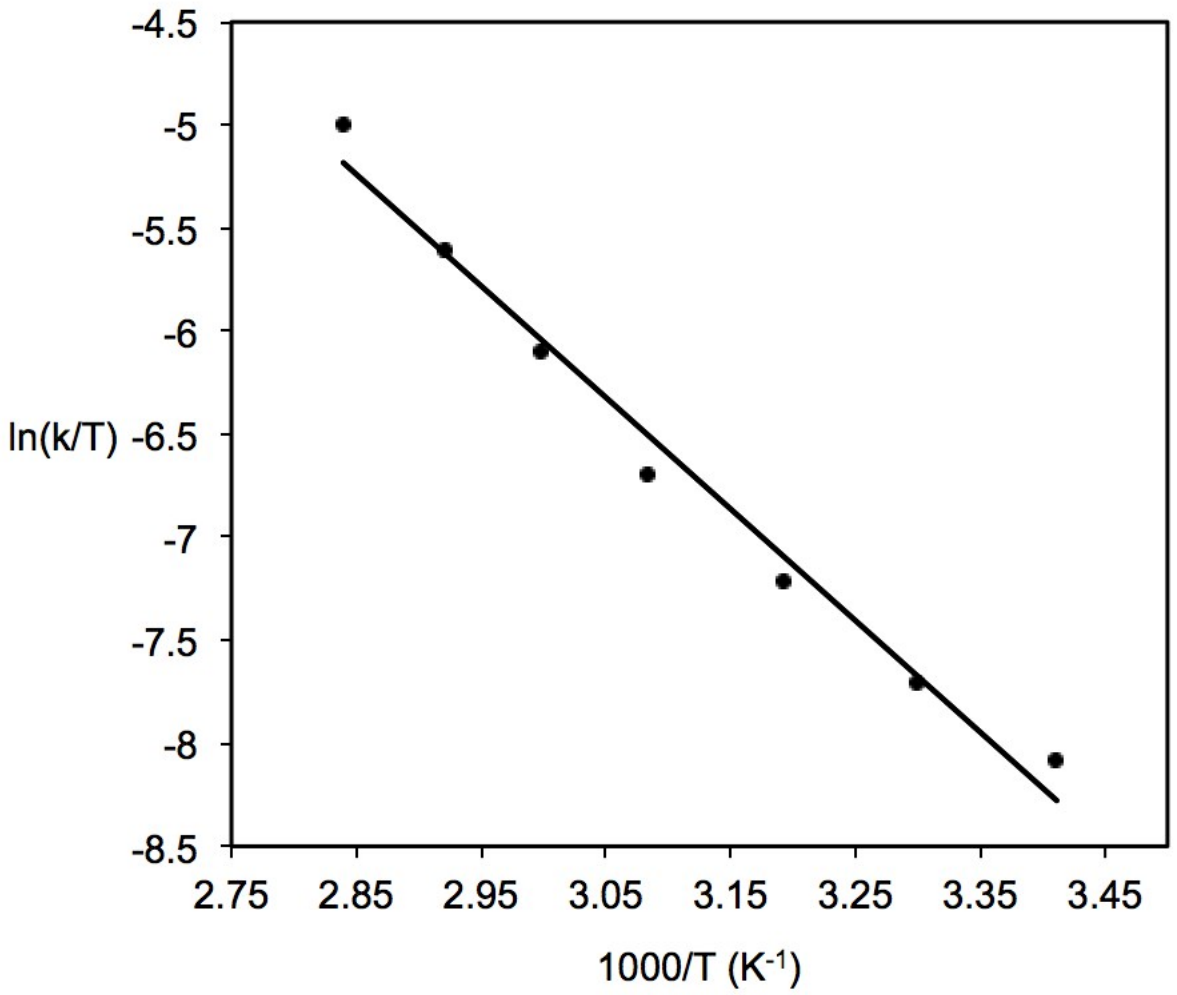

Figure S38. Plot of ln (k/T) vs 1/T for the exchange rate data of 5 in dmso-*d*6.

Derived from ^{1}H inversion-transfer experiments at 20, 30, 40, 51, 60, 69 and 79 °C (**Figures S31** to **S37**). The solid line was calculated using linear regression analysis resulting in a correlation coefficient of 0.983. The slopes and intercepts were used to determine enthalpy ($\Delta H^{\ddagger}$) and entropy ($\Delta S^{\ddagger}$) of activation values of 10.7 ± 0.6 kcal mol^{-1} and -27.0 ± 1.9 cal mol^{-1} K^{-1} respectively, resulting in a free energy of activation ($\Delta G^{\ddagger}$) of 18.8 ± 0.9 kcal mol^{-1} at 298 K.

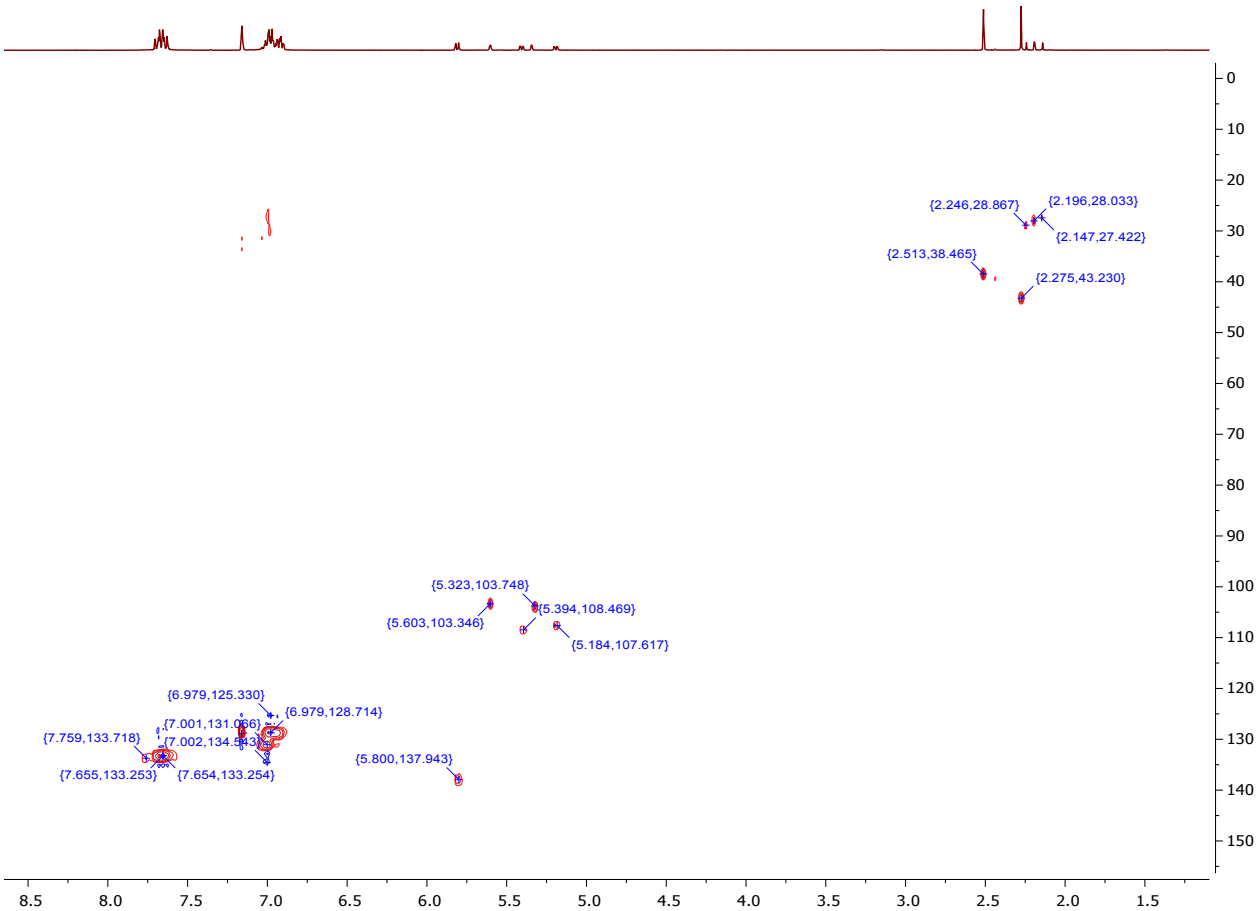

Figure S39. HSQC spectrum of the reaction mixture for the formation of **Bd** in C_6D_6.

References:

1 A. D. Bain and J. A. Cramer, *J. Magn. Reson.*, 1996, **118**, 21–27.

2 J. J. Led and H. J. Gesmar, *J. Magn. Reson.*, 1982, **49**, 444–463.